

**SGP**
FUNDADA 1924**Boletín de la Sociedad Geológica del Perú**journal homepage: www.sgp.org.pe

ISSN 0079-1091

Application of Seismic Stratigraphy for Frontier Hydrocarbon Exploration, Salaverry Basin, Peru: insights into potential reservoirs

Diego Timoteo ¹, Farid Chemale Junior ², Edgar Borda ³¹ Hound Exploration S.A.C, Lima, Peru, diego.timoteo@houndexplo.com² Instituto de Geociências, Universidade de Brasília, Brasília, Brasil³ Savia Perú S.A., Lima, Perú

ABSTRACT

This study is focused in the Salaverry Basin, Peruvian Andes Forearc, which contains three sampled and analyzed oil seeps, suggesting at least one active petroleum system within the basin. It has been developed during Cenozoic in an extensional tectonic setting punctuated by compressive periods controlled by the interaction between Nazca-Farallon and South American plates, and Nazca ridge subduction. Seismic stratigraphic analysis calibrated with available well and core data was applied in order to provide the spatial-temporal evolution of Cenozoic depositional systems in this basin. As a result, the Cenozoic succession in the central portion of Salaverry Basin is best subdivided into eleven seismic stratigraphic sequences (S1-S11), controlled predominantly by tectonism and also by sea-level fluctuations. Afterwards, effective integration of sequences geometry, thickness variations and seismic facies enhanced interpretation of depositional systems and prediction of subsurface lithologies. Thus, this study adds new potential reservoir rocks into the S1, S2, S7 and S8 sequences and seal rocks into the S3, S6, S9-S11 sequences; for the petroleum systems previously defined in the basin. These new petroleum system elements increase the chance of success from many deeply buried prospects that remain to be drilled by exploratory wells, in the central portion of the Salaverry Basin.

RESUMEN

Este trabajo se enfoca en la Cuenca Salaverry, Antearco de los Andes peruanos, la cual contiene tres *oil seeps* muestreados y analizados, sugiriendo la presencia de al menos un sistema petrolero activo dentro de la misma. La cuenca se formó durante el Cenozoico, controlada por procesos extensionales con tectónica compresiva localizada, que están relacionados a la interacción de las placas de Nazca y Sudamericana, y la dorsal de Nazca. Análisis sismoestratigráfico calibrado con datos de pozo y núcleos disponibles, se realizó con el fin de interpretar la evolución de los sistemas deposicionales Cenozoicos. Como resultado, la sucesión Cenozoica en la porción central de la Cuenca Salaverry se dividió en once secuencias estratigráficas sísmicas (S1-S11), controladas predominantemente por tectonismo y también por fluctuaciones del nivel del mar. Luego, la integración efectiva de la geometría de las secuencias, variaciones de espesor y las facies sísmicas mejoraron la interpretación de los sistemas deposicionales y la predicción de litologías en el subsuelo. Ciertamente, este trabajo adiciona nuevas potenciales rocas reservorio en las secuencias S1, S2, S7 y S8; y rocas sello en las secuencias S3, S6, S9-S11, para los sistemas de petróleo previamente definidos en la cuenca. Estos nuevos elementos del sistema de petróleo incrementan las posibilidades de éxito de muchos prospectos exploratorios que aún deben ser perforados, en la parte central de la Cuenca Salaverry.

Palabras claves: Salaverry Basin, Seismic stratigraphy, Hydrocarbon exploration, Forearc Basin, Peruvian margin, Andes.

1. Introduction

Peruvian forearc basins are developed on the western margin of South America and can be divided into two segments. The northwest petroliferous province (Talara, Sechura and Tumbes basins) which has been the focus of exploration and production for more than 100 years, and the south-central province (Salaverry, Trujillo and Lima basins) which has been relatively unexplored (Fig. 1).

This study is focused in the Salaverry basin, which is a frontier exploratory area with major undiscovered resources (Figs. 1 and 2). Furthermore, it contains three sampled and analyzed oil seeps suggesting at least one active petroleum system within the basin (Valencia et al., 2013). Previous exploratory works defined two petroleum systems in the basin: Upper Jurassic Chicama – Cenozoic (.) and Albian La Zorra – Cenozoic (.) (Valencia et al., 2011; 2013).

Thus, they characterized potential Cenozoic reservoirs based on petrophysical studies from well data, and petrographic studies from outcrop and core samples, although without higher detail (Minguito et al., 1997; Wine et al., 2001; Peña, 2011).

Therefore, the present study applies seismic stratigraphic analysis that integrates all the datasets mentioned before, and enhances lithological prediction of reservoir facies within the entire Cenozoic succession. According with that, only two exploratory wells pass through the Cenozoic rocks in the study area: Ballena-1X drilled at the western edge of the Salaverry Basin, and Delfin-1X well drilled at the eastern flank of Trujillo Basin (Figs. 2 and 3). Both wells provide fundamental data in order to calibrate the seismic interpretation (Fig. 4).

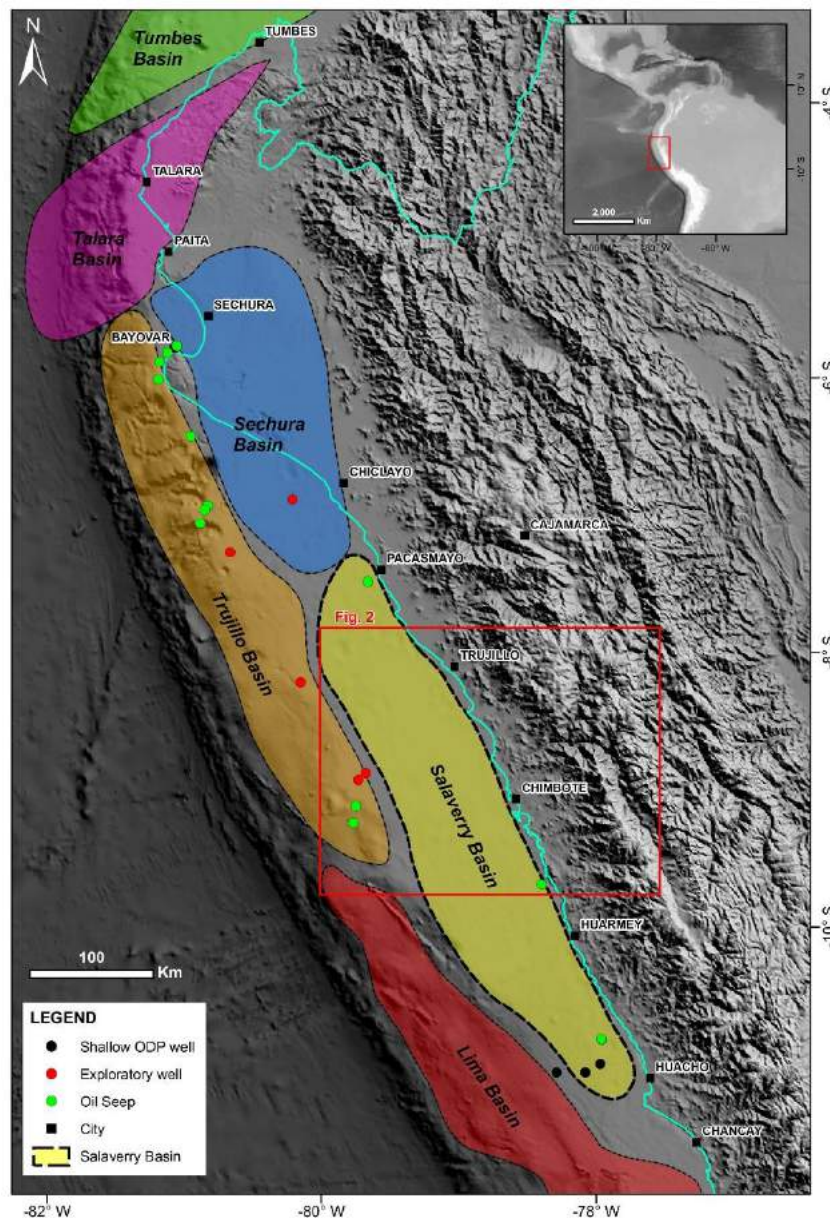


Figura 1. Location map of the Peruvian Forearc petroliferous/tectonic province, comprising the Salaverry Basin (yellow dotted line) and Northwest petroliferous province (Talara, Sechura and Tumbes Basins). The exploratory wells and oil seeps from south-central exploratory province are also indicated.

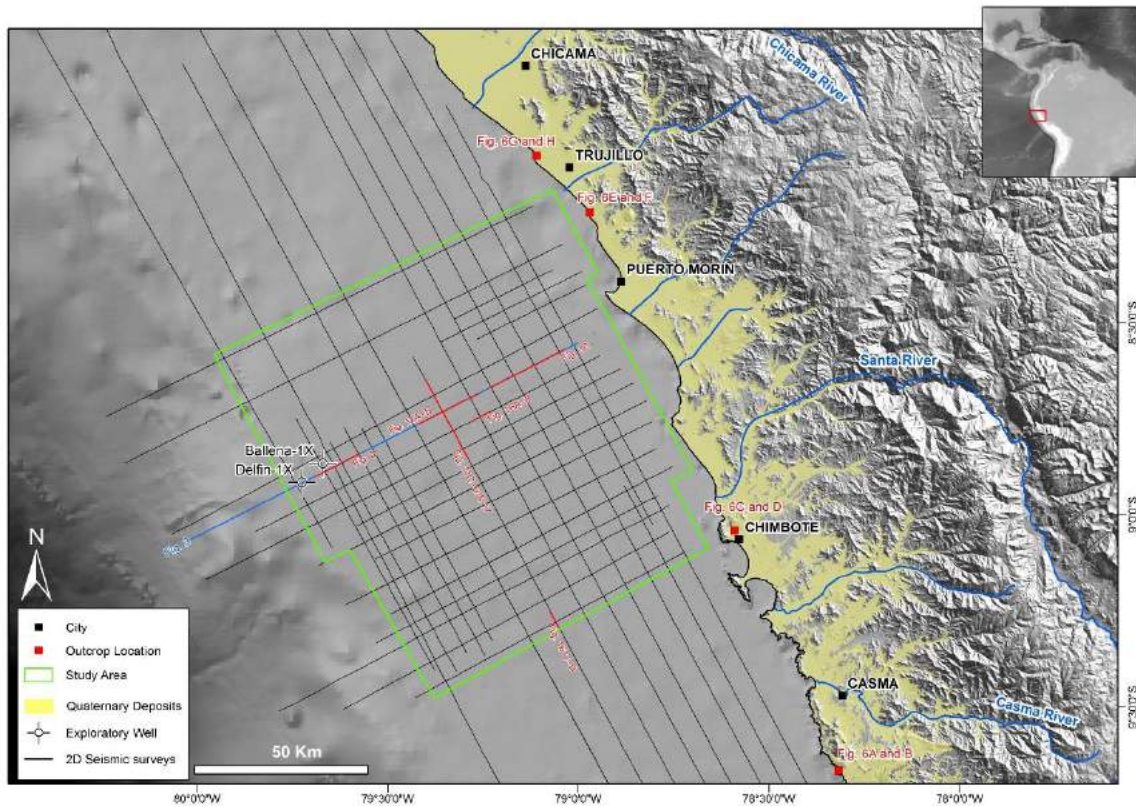


Figura 2. Map of the northern central Peruvian margin showing the location of the study area (green polygon) and its relation with the main fluvial system. The figure also illustrates the location of 2D seismic surveys, and the exploratory wells used in the present study.

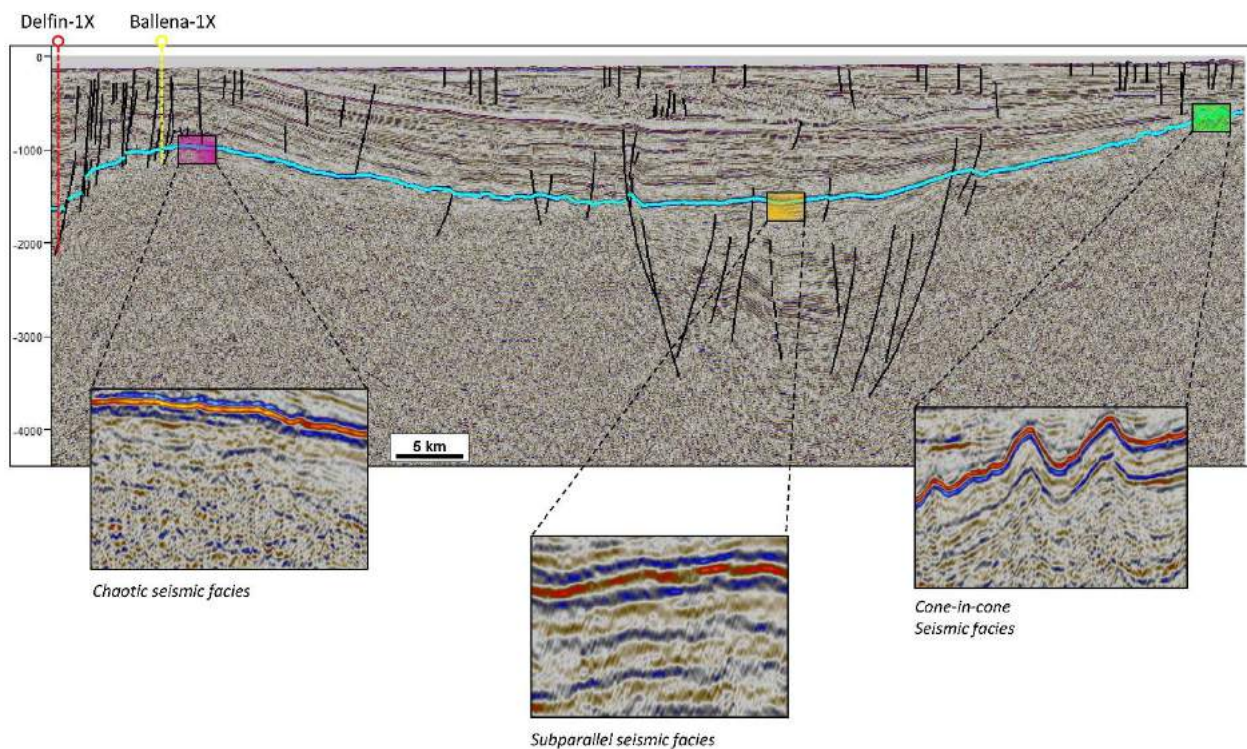


Figura 3. Seismic section showing the Cenozoic sedimentary deposits that overlay the Pre-Cenozoic Basement (PCB). It is composed by different units, as represented by each seismic facies. Moreover, interpreted seismic horizon (cyan) represents the Top PCB. The location of the seismic section and wells is indicated in Fig. 2.

Indeed, this study presents a new application of seismic stratigraphy to a frontier region in shallow water offshore Peru (west South America), where there are great hydrocarbon potentials in the Cenozoic deposits. Because many deeply buried prospects remain to be drilled by exploratory wells, mapping and delineating depositional systems in the subsurface on a regional basis are fundamentally important to the success of exploration programs.

2. Data and Methods

This study is based on regional 2D seismic surveys that accumulate 2831 linear Km covering approximately 11,600 km² of basin area, and two exploratory wells (Fig. 2). The 2D seismic lines are oriented parallel and perpendicular to the peruvian coast. The seismic surveys are time migrated thus the vertical scale is in milliseconds two way time (ms TWT).

Seismic imaging is generally good but quality and resolution decrease over the western margin and where shallow and deep gas indicators (DHIs) are observed (see Timoteo, 2015 for detailed explanation).

Only two exploratory wells were drilled in the study area, specifically over its western edge (Figs. 2, 3 and 4). These wells have a standard wireline log suite comprising gamma ray (GR in API units), spontaneous potential (SP in mv), resistivity (ILD and SN in ohm.m units), sonic (DT in μ s/ft) and density (DEN in g/cm³) logs.

Both cuttings and core samples, and biostratigraphic descriptions are utilized to support interpretation of depositional environments. Stratigraphic age of Cenozoic deposits is based on an integration of micropaleontological, calcareous nannoplankton, and diatomaceous analysis (Valdespino and Seminario, 1976a, 1976b; Schell, 1978; Okada, 1990; Schrader and Cruzado, 1990; Canchaya and Paz, 1992; Narvaez and Pardo, 1993; Morales and Gonzales, 2006). Likewise sonic and density logs, and check-shot surveys were used to generate synthetic seismograms to tie well to seismic (Fig. 5).

In addition, surface data correspond to fieldwork carried out in outcrops along the coast and adjacent to the basin (Figs. 2 and 6).

This study applies standard seismic stratigraphic interpretation workflow (Mitchum et al., 1977; Sangree et al., 1977; Vail et al., 1977, 1987; Veeken, 2013) to figure out the depositional systems and predict lithologies for the Cenozoic units in the central portion of the Salaverry Basin.

Thus, reflection terminations (e.g. onlap, downlap, toplap, offlap, apparent toplap and erosional truncation) are identified and mapped in order to define key seismic discontinuities that bound major seismic stratigraphic sequences across the basin. In the same way, seismic facies are recognized, described and mapped per each seismic stratigraphic sequence; based on reflection configuration (geometry), continuity, amplitude, frequency and the overall external form of the reflection package (Table 1).

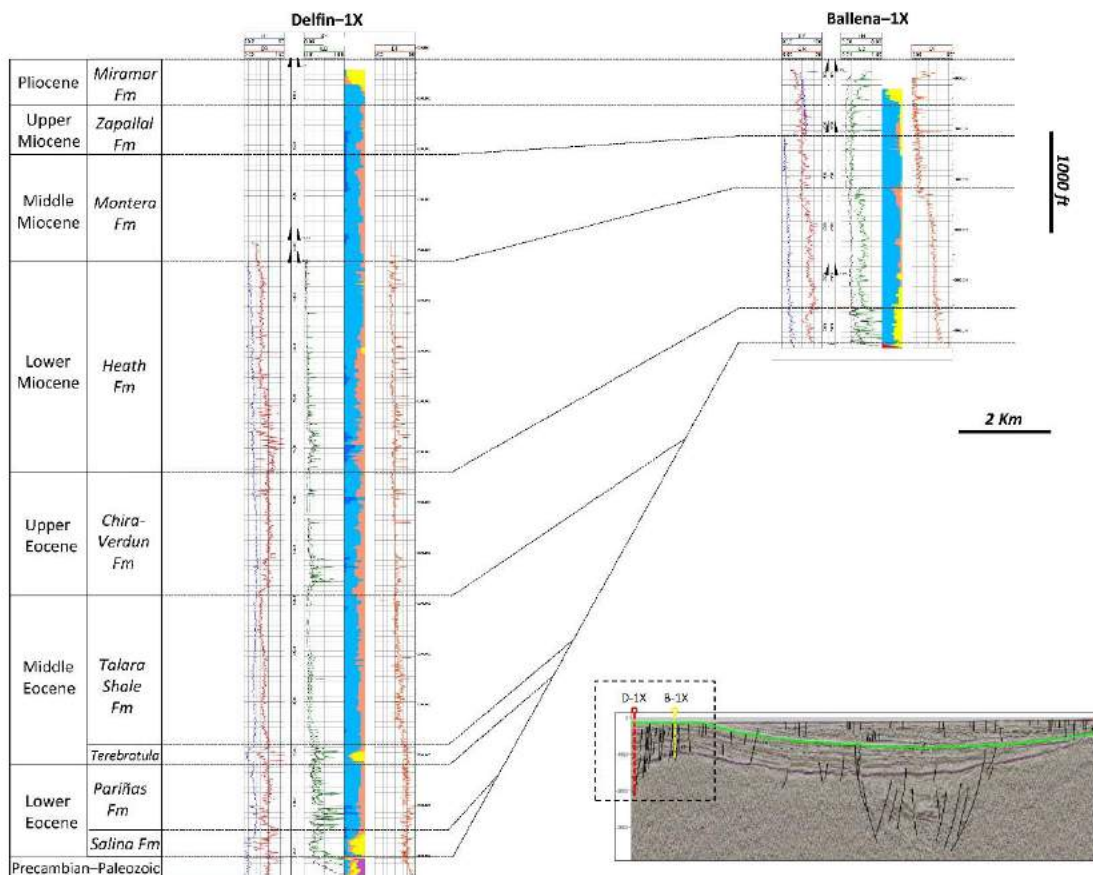


Figura 4. Composite well-log correlation showing the stratigraphic framework in the study area. GR = gamma ray log given in API units; SP = spontaneous potential log given in mv; ILD and SN = resistivity logs given in ohm.m; DT = sonic log given in μ s/ft. In addition, on the lower right corner, the seismic section shows an interpreted horizon (green) which bounding the drilled units and not-drilled Pliocene-Holocene succession. See Fig. 2 for well locations.

3. Geological Setting

The Salaverry basin is located on the western margin of South America over the Peruvian sea and it is part of the forearc domain, which comprises a large petroliferous/tectonic province (Fig. 1). The basin extends from Huacho in northern Lima department to Pacasmayo in La Libertad department, and it covers at least 35,078 km² almost entirely offshore with a small portion onshore (1,200 km²) (Fig. 1).

The origin of the Salaverry basin is associated with the interaction between Nazca-Farallon and South American plates. Active subduction erosion for this margin and subsequent extensional strain controlled the normal faulting and subsidence in Salaverry basin, predominantly over its western margin (Clift et al., 2003; Romero et al., 2011, 2013; Witt et al., 2011). In addition, the Andean orogen uplift controlled the flexural subsidence over the basin axis and the eastern margin (Valencia et al., 2013; Timoteo, 2015). Recent oblique collision of the Nazca aseismic Ridge with the trench caused interplate coupling and its subsequent subduction beneath the South American plate, which began ~15 Ma ago at 9°S (Rosenbaum et al., 2005), dominated the Paracas Arch uplift and also controlled punctuated compressive periods in the forearc region (Gutscher et al., 2000; Hampel, 2002; Rosenbaum et al., 2005; Alemán, 2006; Romero et al., 2013). The Salaverry basin overlies continental-type crust composed by the Paracas Terrane, which have offshore evidences from Precambrian-Paleozoic metamorphic rocks exposed at the Las Hormigas de Afuera Island (west of Lima) and also drilled by exploratory wells (Ramos, 2014; Timoteo, 2015).

The boundaries of Salaverry basin are well defined and it is impossible to describe the basin without the interaction with at least two other basins, the Trujillo basin to the west and the Sechura basin to the north (Fig. 1). Nowadays, the Salaverry basin is separated from the Trujillo basin to the west by the Paracas Arch (Fig. 7), a submerged structural high of much larger metamorphic blocks (Kulm et al., 1981; Ramos and Aleman, 2000). The present-day eastern margin is bounded by the coastline and Mesozoic rocks exposed along the coast (Fig. 7A). However, the Salaverry basin was not always isolated from nearby basins. Intermittent activity along normal faults that dominated basement structural highs may have controlled interactions between the Salaverry, Trujillo, Sechura and Lima basins.

Thus, the Cenozoic Salaverry Basin has been developed over Pale-Mesozoic rocks that conforms the ancient Peruvian continental margin basin (Romero et al., 2010; 2011) (Fig. 3). The following section describes the Cenozoic stratigraphic record in the basin and remarks the Pre-Cenozoic Basement that underlies it. It is necessary to mention that the study area is located in the central portion of the Salaverry Basin, between latitudes 8° S - 9° 30' S (Fig. 2).

3.1. Pre-Cenozoic Basement (PCB)

It corresponds to the different sedimentary, volcano-sedimentary, metamorphic and igneous units that underlie

the Cenozoic sedimentary succession in the basin (Fig. 3). The geographic extent of each unit differs across the basin and mostly is interpreted according to the integration of well, seismic, geopotential and surface geological data (see Valencia et al., 2011; Timoteo, 2013; 2015 for detailed explanation). These Pre-Cenozoic rocks act as the basement and they are important because correspond to potential elements of petroleum systems in the Salaverry basin (Timoteo, 2013; 2015). Thus, the Upper Jurassic and Albian marine black shales are relevant due to they are characterized as potential source rocks (Valencia et al., 2011).

3.2. Stratigraphic Framework

In the study area, the Cenozoic stratigraphic record reaches ~2 km thickness and is derived from data of Ballena-1X and Delfin-1X exploratory wells, and coastal outcrops preserved onshore (Figs. 2, 3, 4 and 6). Biostratigraphic revision allowed updates the age from stratigraphic units and improves the well-log correlation. As a result, the oldest unit corresponds to the Lower Eocene and has been drilled over the eastern flank of the Trujillo basin whereas in the Salaverry basin there is record from the Upper Eocene to the basal Pliocene. Moreover, the thickest Pliocene-Holocene succession has not been drilling yet in the basin (Fig. 4).

The Upper Eocene Verdun Formation rests unconformably on Pre-Cenozoic metamorphic and volcano-sedimentary rocks of the Paracas Arch and Casma Group, respectively (Fig. 3). The Verdun Formation is comprised by planar cross-bedded quartz sandstones intercalated with claystones, which contain abundant shell fragments and is consistently barren of micropaleontological species. This formation has been interpreted as deltaic/shelf deposit (Fig. 5).

Upsection, a significant unconformity separates the Verdun Formation from the Lower Miocene Heath Formation. The Heath Formation consists of fine-grained quartz sandstones at the base, overlain by claystones intercalated with siltstones. Based on its stacking patterns, biofacies associations and paleobathymetry (Okada, 1990; Canchanya, 1992), this formation has been interpreted to represent a shallow marine deposit deepening upsection onto deep marine deposits (Fig. 5).

Upsection, an unconformity and a superimposed marine flooding event separates the Heath Formation from the Middle Miocene Montera Formation. The Montera Formation predominantly comprises claystones intercalated with siltstones and some layers of fine-grained quartz sandstones, which has been interpreted as deep marine deposit (Fig. 5).

Following upward in the stratigraphic succession, the Upper Miocene Zapallal Formation conformably overlies the Montera Formation. The Zapallal Formation is predominantly comprised of claystones intercalated with very fine sandstones and siltstones; which contain foram microfossils, calcareous nannofossils and siliceous microfossils (Okada, 1990; Schrader and Cruzado, 1990; Canchanya and Paz, 1992). Based on its biofacies associations this formation has been interpreted as an outer shelf marine deposit (Fig. 5).

Towards the top of the stratigraphic section, the Pliocene–Holocene succession conformably overlies the Zapallal Formation. This succession consists of Miramar and Hornillos Formations. Likewise, the Miramar basal section only has been drilled by Ballena–1X and Delfin–1X exploratory wells while the thickest section of the Pliocene–Holocene succession has not been drilled yet in the basin (see the seismic section in Fig. 4). Thus, the basal section of Miramar Formation consists of conglomeratic sandstones intercalated with some layers of claystones, interpreted as shallow marine deposit that shallows upsection (Fig. 5).

Furthermore, the uppermost section from the not-drilled Pliocene - Holocene succession would correspond to the sedimentary deposits exposed along the coast and adjacent to the basin (Fig. 2).

Fieldwork carried out between latitudes 8° S - 9° 30' S allowed recognize: fluvial-alluvial deposits at the southern end of the study area, shoreface deposits at Chimbote, aeolian deposits at Salaverry, and alluvial fan deposits at Huanchaco on the northern end of the study area (see Peña, 2011 for detailed explanation) (Fig. 6). As the formal stratigraphic nomenclature for the Cenozoic units in the study area has not been published, the present work follows the stratigraphic subdivisions from Dunbar et al. (1990), Minguito et al. (1997), Martinez et al. (2005), Deckelman et al. (2008), and Gonzales (2014); which are based on more recent seismic, well, field and biostratigraphic data. The Eocene to Holocene siliciclastic succession described before has been fed by major fluvial systems from eastern Andean region such as Santa, Casma and Chicama rivers (Fig. 2).

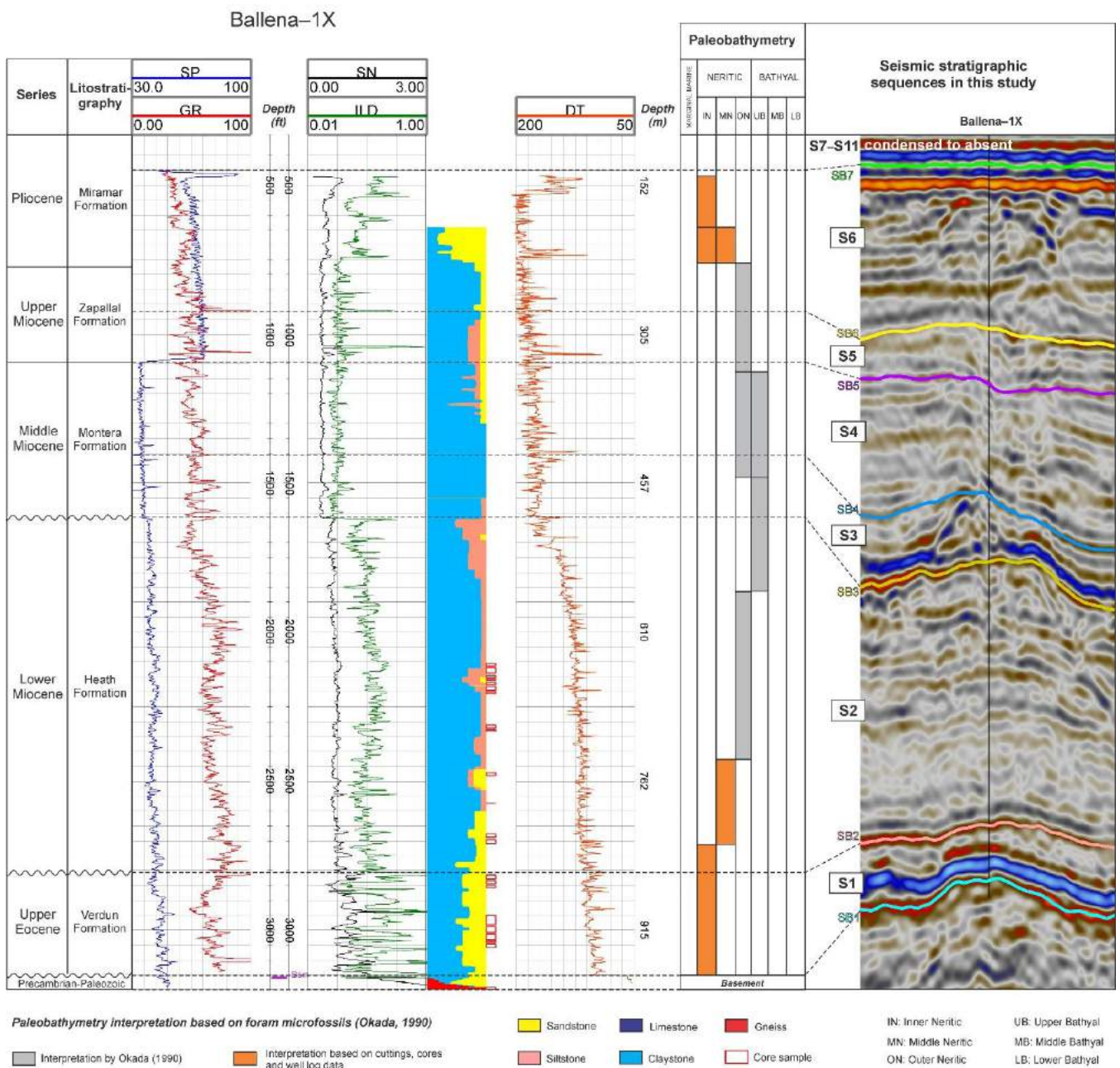


Figura 5. Lithostratigraphic subdivisions of the Cenozoic succession in the central portion of Salaverry Basin and the corresponding seismostratigraphic units interpreted in this study. See Fig. 2 for well location.

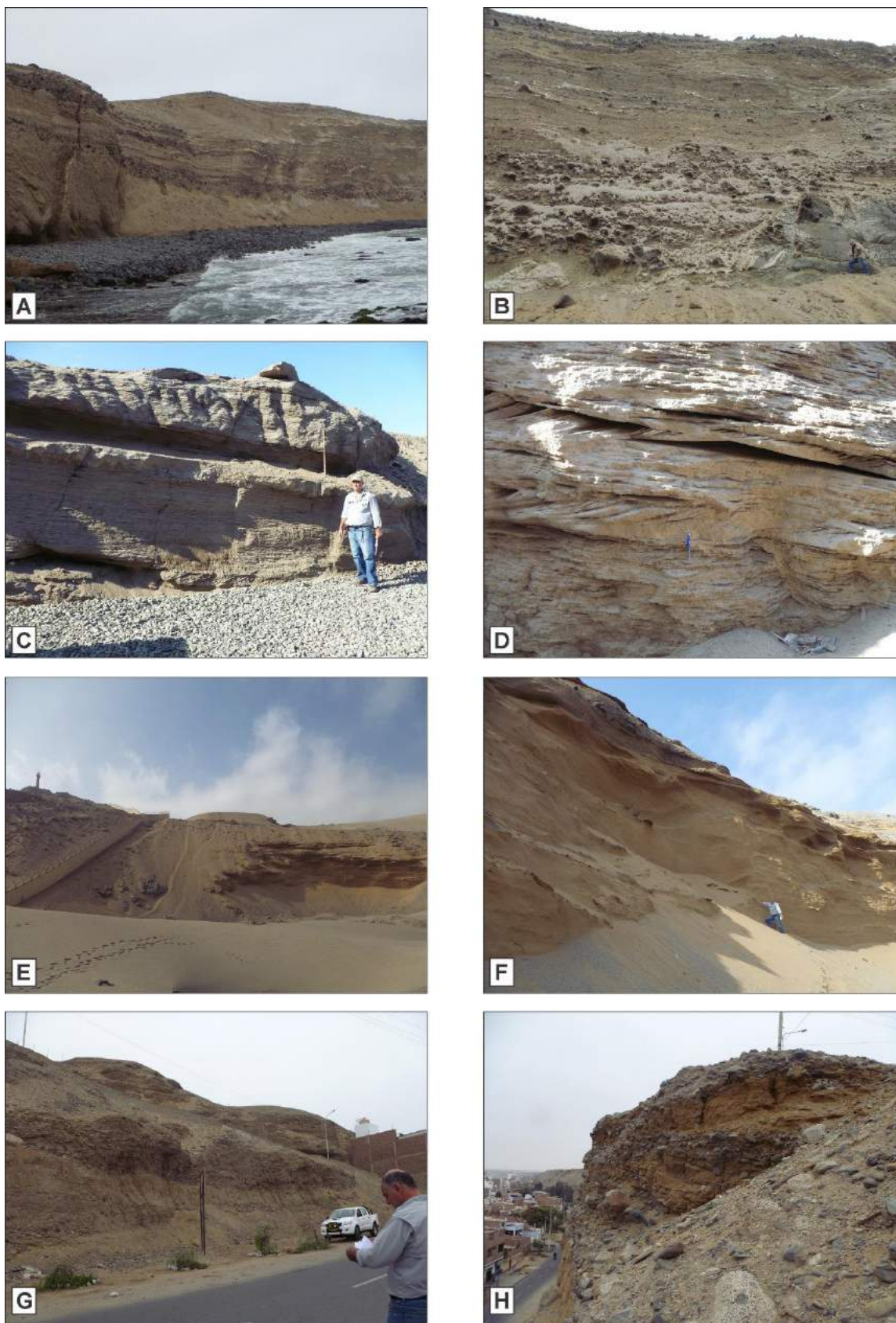


Figura 6. Sedimentary deposits exposed along the coast and adjacent to the basin. A) and B) Fluvial-alluvial deposits overlay unconformably on Upper Cretaceous volcanic rocks. C) and D) Shoreface deposits comprised by low angle cross bedded sandstones and sandstones with wavy ripples. E) and F) Aeolian deposits overlay unconformably on granites from Coastal Batholith. G) and H) Alluvial fan deposits comprised by debris flow, channel and bars intercalated along the section; its base is not exposed. See Fig. 2 for outcrop locations.

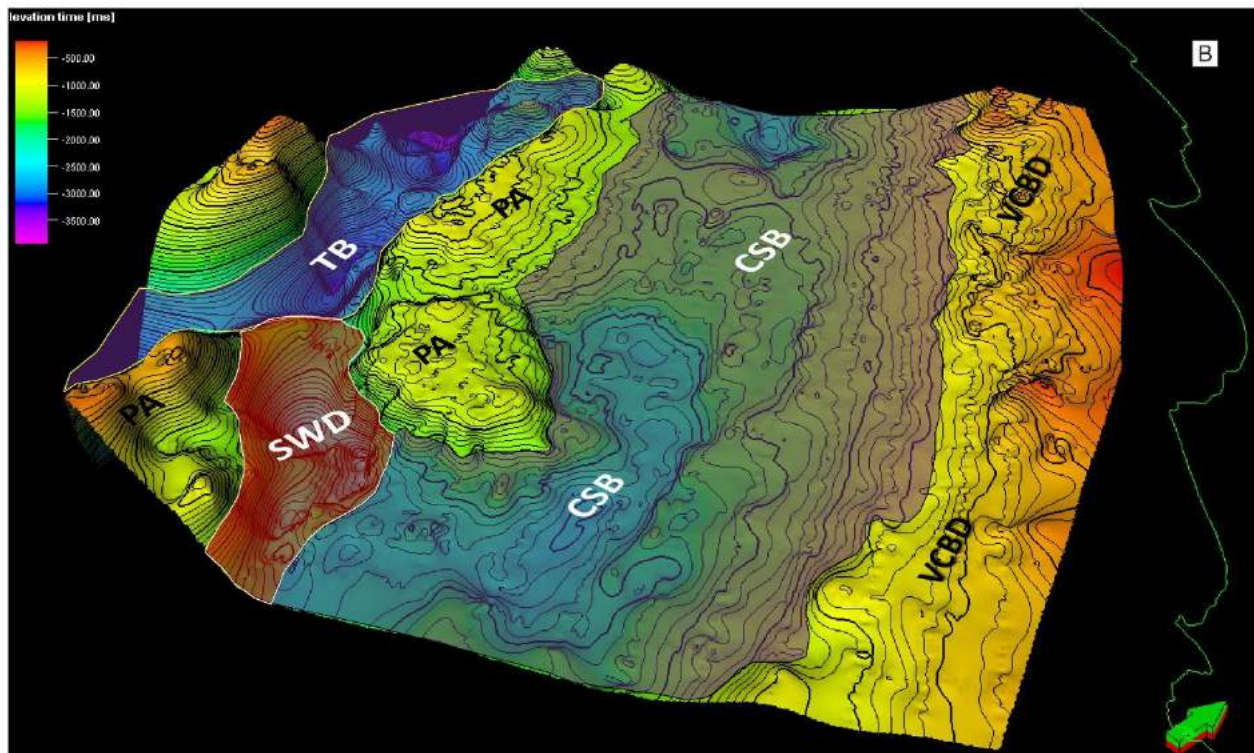
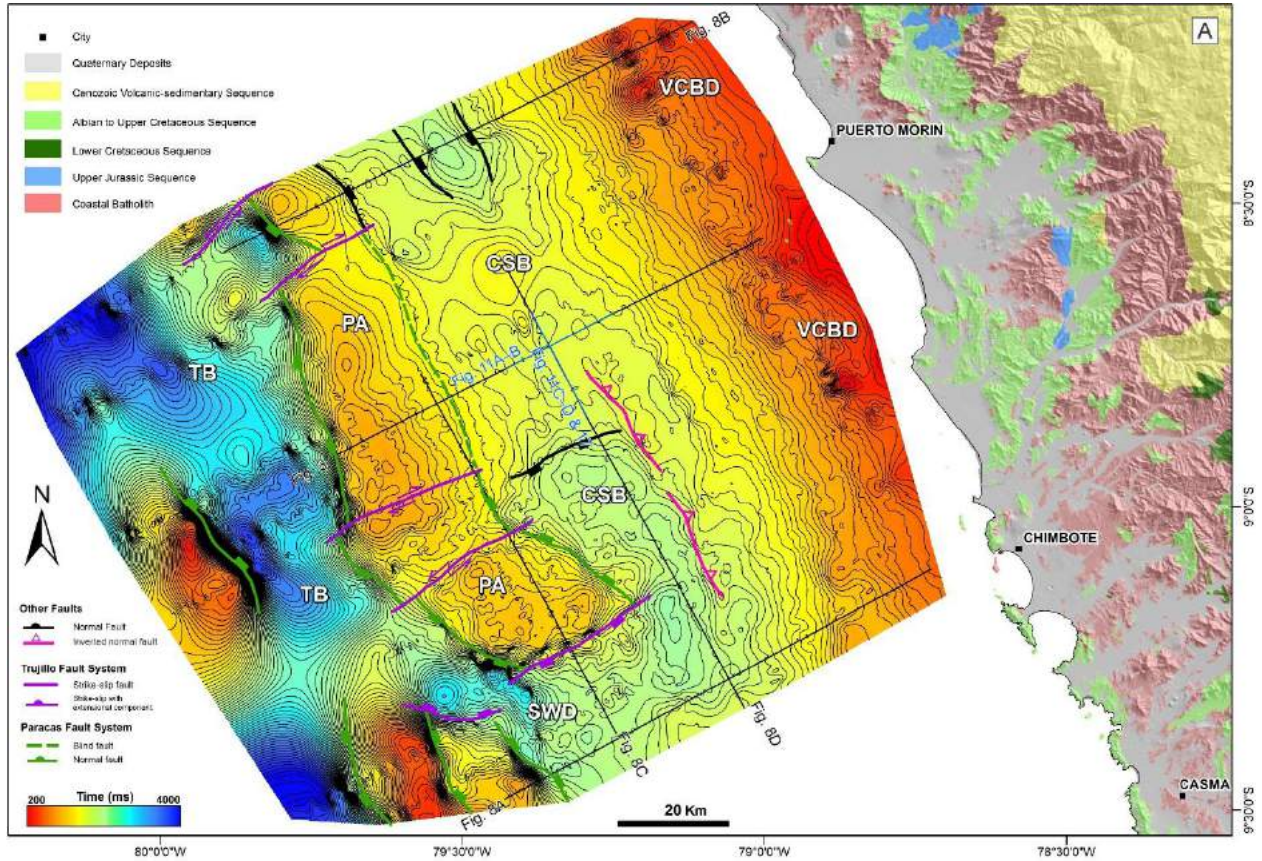


Figura 7. A) Time structure map of the Top Pre-Cenozoic Basement showing the main fault systems and the morphostructural domains in the study area. Contour lines are every 50 ms. TB = Trujillo Basin; PA = Paracas Arch; CSB = Cenozoic Salaverry Basin; VCB = Volcanic arc and Coastal Batholith Domain, SWD = Southwestern Depocentre. B) 3D perspective view showing morphostructural domains in the study area. The coastline is outlined by the green line.

4. Structural Framework

The Cenozoic Salaverry basin has been developed in an extensional tectonic setting punctuated by compressive periods over Paleo-Mesozoic rocks that act as its basement. Likewise, these Pre-Cenozoic rocks conform the ancient Peruvian continental margin basin, which also evolved during an extensional tectonic regime associated to eastern volcanic arc (Azalgará, 1993; Benavides, 1999; Romero et al., 2010, 2011; Valencia et al., 2011). In this context, the Salaverry basin consists of depocentres and structural highs developed during Eocene-Pleistocene collision between Nazca-Farallon and South American Plates.

The seismic interpretation of the Top Pre-Cenozoic basement in the study area (8° S - 9° 30' S) allows to recognize the Trujillo basin to the west and the Salaverry basin to the east (Fig. 7). Both basins are bounded by a prominent structural high known as the Paracas Arch (Kulm et al., 1981; Ramos and Aleman, 2000) and they are locally linked in the southern part of the study area, called as the southwestern depocentre (SWD) (Fig. 7). The Paracas Arch acts as current western margin of the Salaverry Basin whereas the coastline acts as current eastern flank. Over the eastern margin, concentric morphological features arranged along NW-SE trend correspond to the offshore extension of volcanic arc and Coastal Batholith domain (VCBD) (Fig. 7).

Trujillo is deeper than Salaverry due to its formation and fill began before during Early Eocene (Fig. 4). Later during Middle Eocene the tectonically driven subsidence was only active in Trujillo basin and then during the Late Eocene the subsidence extended eastward generating the initial stage of the Salaverry basin formation, which permitted accumulation of shallow marine deposits resting unconformably onto the PCB (Figs. 4, 5, 8 and 9). Continuous extensional regime since the Early Eocene with subsidence predominantly controlled by normal faulting was related to subduction erosion (Von Huene and Scholl, 1991; Clift et al., 2003; Romero et al., 2013). The Salaverry basin subsided considerably and was filled during the Late Eocene-Oligocene but a "Terminal Oligocene event" modified the basin geodynamics, triggering the erosion of the entire Oligocene succession and the uppermost section from the Upper Eocene rocks (Figs. 4 and 5).

The structural seismic interpretation allows to recognize three main fault systems in the study area (Figs. 7A and 8).

The "Paracas fault system", comprised of major NW-SE trending normal faults with east and west vergence. Most of them cut the PCB and younger rocks while others correspond to blind faults that do not reach the Cenozoic sequence (Figs. 7, 8A and 8B).

The "Trujillo fault system", comprised of major NE-SW trending strike-slip faults. They correspond mainly to sinistral and dextral strike-slip faults as well as some strike-slip faults with extensional component at the SWD margins (Figs. 7A and 8C).

On the other hand, several minor normal faults, with east and west vergence, are seen across the basin foredeep and conform the "Interior fault system" (Figs. 7 and 8D). Most of them cut the Cenozoic sequence (Fig. 8A and D) whereas some pass through the sedimentary succession and reach

the PCB (Fig. 8B and D). Moreover, exceptional structural setting (compression and partial inversion of previous structures) is seen in the study area and is related to local compressive events product of Nazca Ridge subduction beneath South American plate (Timoteo, 2015) (Fig. 7A).

5. Seismic Stratigraphy

Seismic stratigraphic analysis calibrated with available well and core data was applied to figure out depositional systems and predict lithologies in the study area. As a result, twelve seismic sequence boundaries (SB1 - SB12) and twelve seismic facies (SF1 - SF12) were identified and mapped throughout the Cenozoic sedimentary succession (Fig. 8; Table 1). These seismic sequence boundaries, together with major changes in seismic facies, define eleven seismic stratigraphic sequences: S1 - S11. Thus, the following section describes the key seismic horizons and the seismic sequences they define (see the stratigraphic panel in Fig. 8).

5.1. Seismic sequence boundaries

Through the reflection termination mapping has been recognized discontinuity surfaces interpreted as unconformities or correlative conformities. These seismic horizons correspond to sequence boundaries that define the stratigraphic framework in the study area (Fig. 8).

SB1 (cyan)

The SB1 reflection is continuous and characterized by a strong peak. Well to seismic tie indicates that SB1 coincides with the top Pre-Cenozoic Basement and thus represents a major regional unconformity all over the basin (Figs. 5, 9 and 10). The SB1 is also locally disrupted by several igneous intrusions and volcanic extrusions over the VCBD (Figs. 7 and 8B). Moreover, the SB1 is cut by Paracas, Trujillo and Interior fault systems; some of these faults propagate into the Cenozoic succession (Fig. 8).

SB2 (salmon)

The SB2 corresponds to a regional unconformity based on biostratigraphic, well log and seismic data and represents a strong gap in the sedimentary record between the Upper Eocene and Lower Miocene rocks (Fig. 5). It is a relatively continuous seismic horizon composed by a moderate peak, is only present over the western margin of the basin and terminates against the SB1 (Figs. 8 and 9).

SB3 (light yellow)

The SB3 has been mapped consistently over the west and south sectors of study area. This seismic horizon evidence a strong discontinuity and a superimposed marine flooding event between Lower and Middle Miocene deposits over the western margin (Fig. 5), whereas is conformable over the deepest parts of the basin. In this way, the SB3 represents an unconformity and its corresponding correlative conformity (Figs. 5, 8 and 9).

SB4 (light blue)

The SB4 reflection is relatively continuous and composed by a moderate to strong peak (Fig. 5). It is marked by

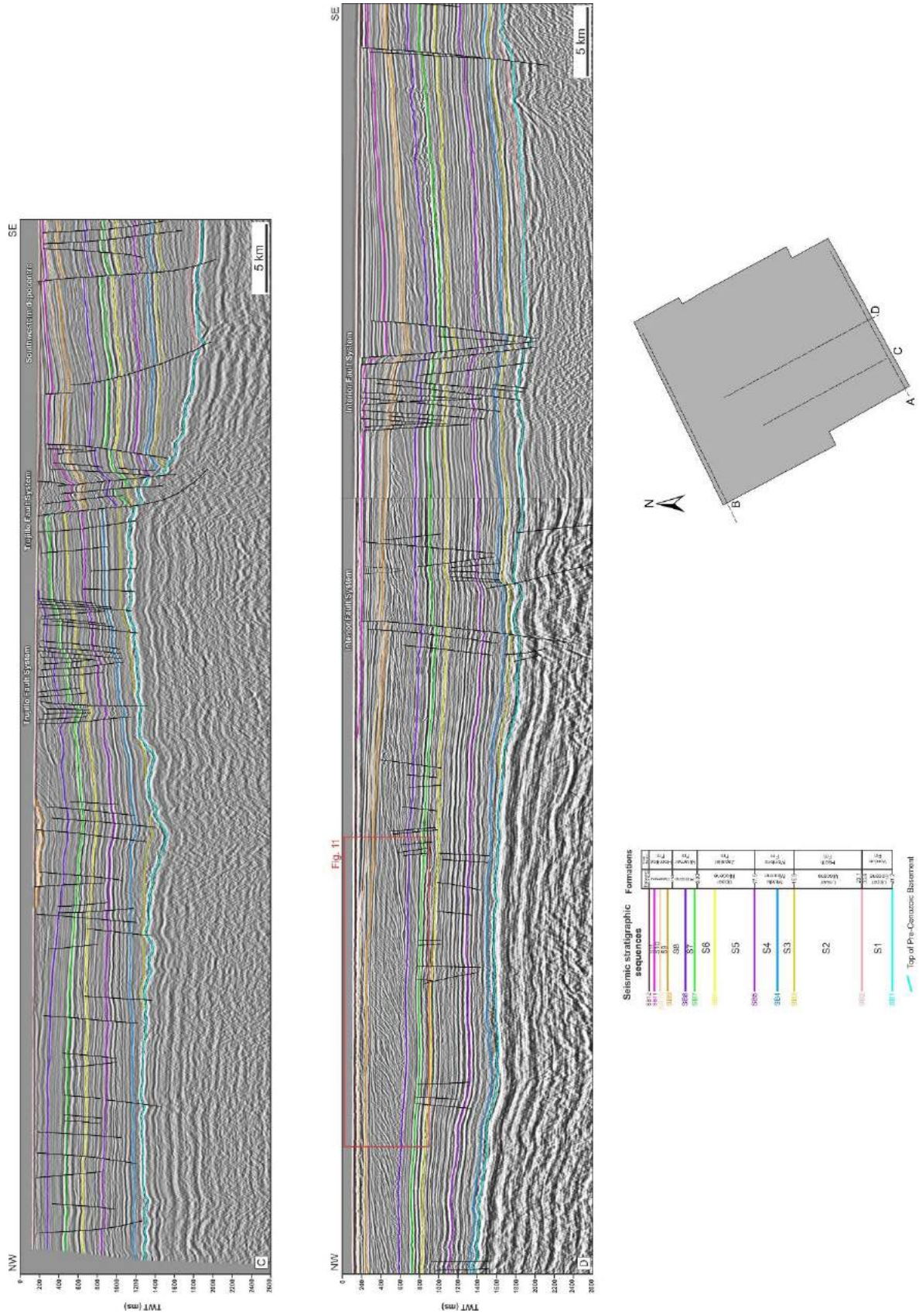


Figura 8. (continued).

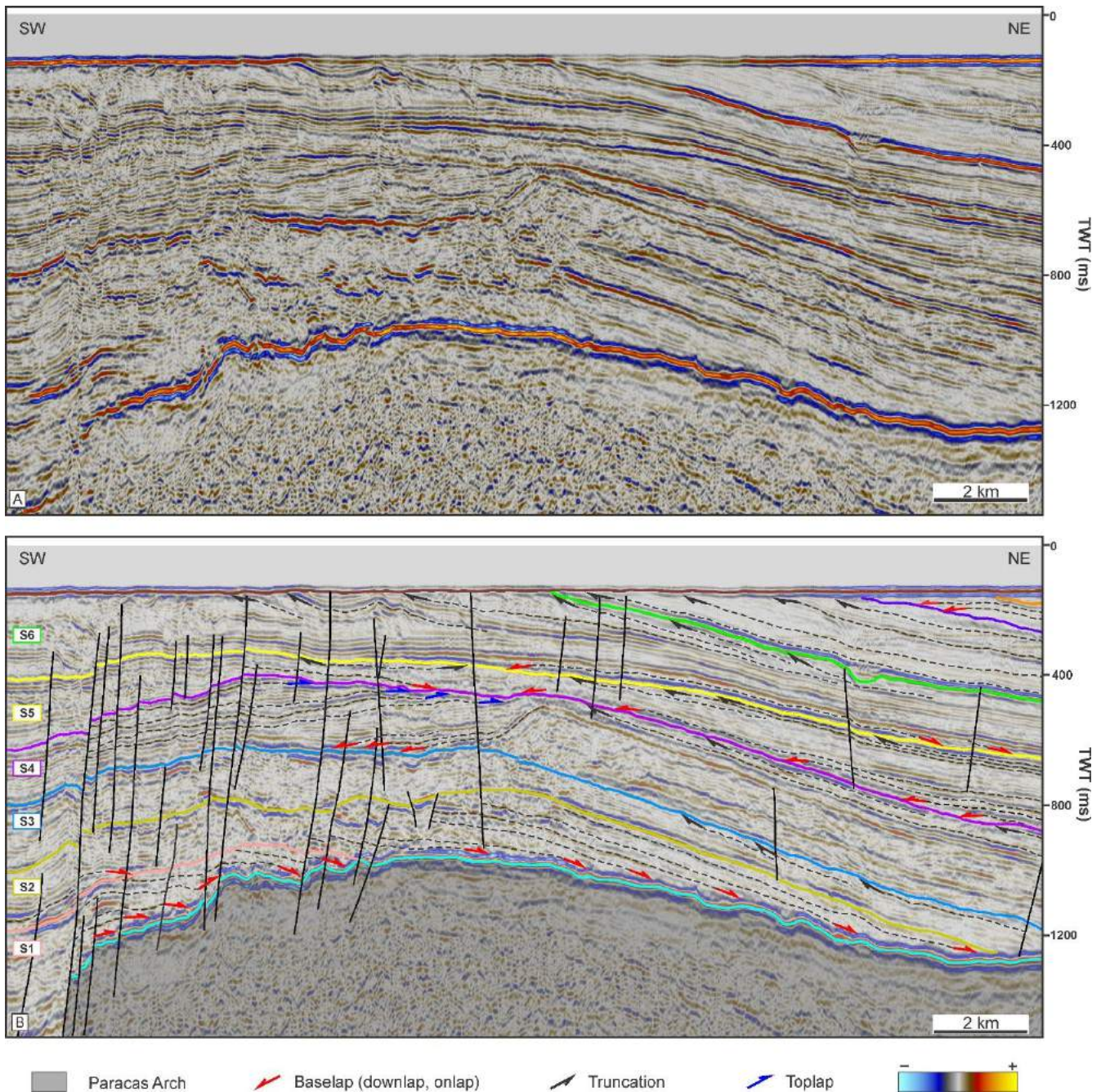


Figura 9. Reflection configuration and terminations within the Cenozoic seismic sequences. A) Uninterpreted and B) interpreted 2D seismic section across the western margin of the basin over the Paracas Arch. The location of the seismic section is indicated in Fig. 2. Legend as in Fig. 8.

truncation and concordant reflections below and baselap above, which evidence a local unconformity on the western margin (Fig. 9) whereas is conformable over the eastern margin and the deepest parts of the basin (Fig. 8).

SB5 (purple)

The SB5 seismic horizon is characterized by a continuous and moderate peak. It is conformable over the basin foredeep and the eastern margin whereas is marked by toplap and truncation below, and downlap above on the western margin (Figs. 9 and 10). The SB5 extends almost all over the study area and represents an unconformity and its corresponding correlative conformity (Fig. 8).

SB6 (yellow)

The SB6 reflection is a moderate to strong peak with consistent lateral continuity. This seismic horizon is marked by truncation below and baselap above which evidence a regional unconformity (Figs. 9 and 10). It terminates against the SB1 over the eastern margin (Figs. 8B and 10).

SB7 (green)

The SB7 has been mapped consistently over the whole study area (Fig. 8). This seismic horizon is a continuous and strong peak marked by truncation and toplap below and concordant reflections above which represent an

Table 1
Seismic facies identified in the Cenozoic succession of the Salaverry Basin. Scale bar is 100 ms.

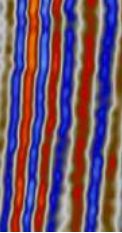


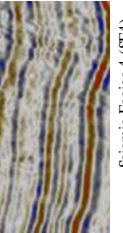
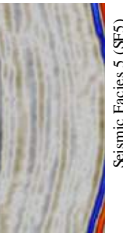
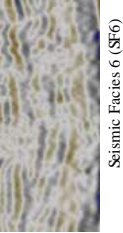
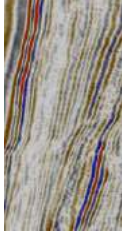
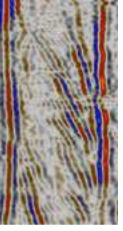
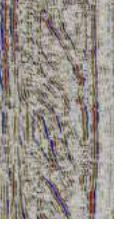
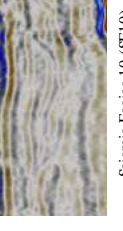
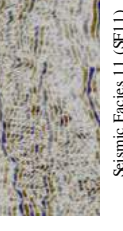
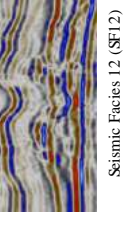
Seismic Facies (SF)	Characteristics	Geological interpretation
 Seismic Facies 1 (SF1)	Parallel, high continuity, high amplitude reflections	Distal sandy turbidites
 Seismic Facies 2 (SF2)	Parallel, high continuity, low to high amplitude reflections	Pelagic/hemipelagic deposits with sandy turbidites
 Seismic Facies 3 (SF3)	Parallel to subparallel, good continuity, low amplitude reflections	Pelagic/hemipelagic deposits
 Seismic Facies 4 (SF4)	Parallel to subparallel, continuous and disrupted in part, low to high amplitude reflections with sheet drape-shaped external form	Pelagic/hemipelagic rocks interbedded with sandy turbidites, related to bottoms currents
 Seismic Facies 5 (SF5)	Parallel to subparallel, continuous and disrupted in part, low to very low amplitude reflections with sheet drape-shaped external form	Pelagic/hemipelagic deposits related to bottoms currents
 Seismic Facies 6 (SF6)	Subparallel, poor to low continuity, variable amplitude reflections with wedge-shaped external form	Fluvial or deltaic plain deposits
 Seismic Facies 7 (SF7)	Divergent, good to low continuity, low to high amplitude reflections with wedge-shaped external form	Marine syntectonic deposits
 Seismic Facies 8 (SF8)	Sigmoid/oblique-shaped clinoforms, with low to high amplitude and intermediate frequency reflections	Deltaic or slope channel fill deposits
 Seismic Facies 9 (SF9)	Concave upward-shaped clinoforms, with low to high amplitude and high to intermediate frequency reflections	Shelfal progradation deposits
 Seismic Facies 10 (SF10)	Hummocky-shaped clinoforms, with low to moderate amplitude and intermediate to low frequency	Shallow marine deposits
 Seismic Facies 11 (SF11)	Chaotic and contorted, very discontinuous, low to high amplitude, intermediate to low frequency	Mass transport deposits
 Seismic Facies 12 (SF12)	Mounded, good to low continuity, low to high amplitude reflections	Siliciclastic or carbonate? buildups

Table 1 (continued)

unconformity and its corresponding correlative conformity (Figs. 9 and 10).

SB8 (blue)

The SB8 reflection represents a major unconformity along the study area. Typically, it is characterized by a moderate to strong peak marked by regional downlap above and local toplap and truncation below (Figs. 10 and 11).

SB9 (orange)

The SB9 seismic horizon is a moderate peak with consistent lateral continuity. Likewise, it is marked by toplap below and baselap above which evidence a regional unconformity (Figs. 10 and 11).

SB10 (peach orange)

The SB10 reflection is characterized by a moderate peak with consistent lateral continuity. It represents an unconformity marked by toplap below and baselap above (Figs. 10 and 11).

SB11 (magenta)

The SB11 seismic horizon is a continuous moderate peak marked by truncation and concordant reflections below, and consistent baselap above which evidence an unconformity (Fig. 10).

SB12 (brown)

The SB12 is nearly parallel to the seafloor and is characterized by a continuous strong peak. It is marked by truncation below and concordant reflections above corresponding to an unconformity (Figs. 9, 10 and 11). This seismic horizon is mainly developed to the east and south sectors of the study area (Fig. 13).

5.2. Seismic Facies

Twelve distinct seismic facies (SF1–SF12; Table 1) were recognized throughout the central portion of the Salaverry Basin based on reflection configuration (geometry), continuity, amplitude, frequency and the overall exterior form of the reflection package (Mitchum et al., 1977; Sangree et al., Ramsayer, 1979; Snedden et al., 2008).

SF1 is characterized by well-stratified, high continuity and high amplitude reflections. It is interpreted as representing distal sandy turbidites.

SF2 shows parallel low to high amplitude reflections with high continuity and is interpreted to comprise pelagic/hemipelagic deposits interbedded with sandy turbidites.

Well-stratified, continuous, low amplitude reflections characterize SF3, which is interpreted as pelagic/hemipelagic deposits.

SF4, characterized by continuous and disrupted in part, low to high amplitude reflections, is interpreted to comprise pelagic/hemipelagic rocks interbedded with sandy turbidites related to bottoms currents.

SF5 consists of continuous and disrupted in part, low to very low amplitude reflections with concordant upper and lower boundaries that form sheet drape bodies. It is

interpreted as representing pelagic/hemipelagic deposits related to bottoms currents.

SF6 is characterized by reflections with poor to low continuity, variable amplitude and intermediate to low frequency. It conforms reflection packages with wedge and sheet drape external forms. SF6 is interpreted as fluvial or deltaic plain deposits.

SF7 shows divergent low to high amplitude reflections with good continuity, which evidence wedge-shaped reflection packages. SF7 suggest lateral variations in the deposition rate or progressive sin-sedimentary uplift of the Paracas Arch (see S5 and S6 sequences in Figs. 12 and 13, respectively).

SF8 is characterized by sigmoid/oblique-shaped clinofolds with low to high amplitude and intermediate frequency internal character. These clinofolds are relatively continuous and internally the reflections are quiet discontinuous with high amplitude at bottomsets. It is interpreted as deltaic deposits (see S8 and S9 sequence in Fig. 13) or slope channel fill deposits (see S4 sequence in Fig. 12).

Relatively continuous concave upward-shaped clinofolds with low to high amplitude and high to intermediate frequency internal character characterizes SF9. Internally the reflections are quiet discontinuous and also single and clustered high amplitudes are recognized at foresets and bottomsets (Fig. 11). The SF9 clinofolds are arranged in fan bodies and they are interpreted as shelfal progradation deposits (see Johannessen and Steel, 2005; Steel et al., 2008 for and overview) (Fig. 11).

SF10 consists of irregular discontinuous, subparallel, low to moderate amplitude reflections forming a hummocky clinofold pattern marked by nonsystematic reflection terminations. It is interpreted as representing shallow marine deposits likely related to deltaic/shelf environment.

Chaotic and contorted discontinuous reflections, with low to high amplitude and intermediate to low frequency characterize SF11. Internally, short segments may occur in contorted, discordant and low subparallel patterns. SF11 is interpreted as mass transport deposits, which can be formed by various mechanisms, i.e. slides, slumps, debris flows (see S1–S4 and S6 sequences in Figs. 12 and 13, respectively).

SF12 is characterized by mounded reflections with low to high amplitude. Internally, the reflections are relatively discontinuous and bursts of high amplitude are recognized at its base. It is interpreted to comprise siliciclastic or carbonate? buildups (see S7 sequence in Fig. 13).

5.3. Seismic Sequences

Seismic sequence S1

The S1 second-order sequence is bounded at its base by SB1 (cyan) and at its top by SB2 (salmon) (Figs. 5 and 8). It comprises the Verdun Formation ranging in age within the Upper Eocene (~ 41.2 – 34.5 Ma) (Fig. 5). In the SWD Middle Eocene deposits are recognized, but poor quality seismic data preclude detailed seismic interpretation thus they are considered as part of S1 (Fig. 8A). Westward, S1 onlaps onto the PCB and the Paracas Arch to the south and north, respectively (Figs. 8A and 9). The areal extent of S1

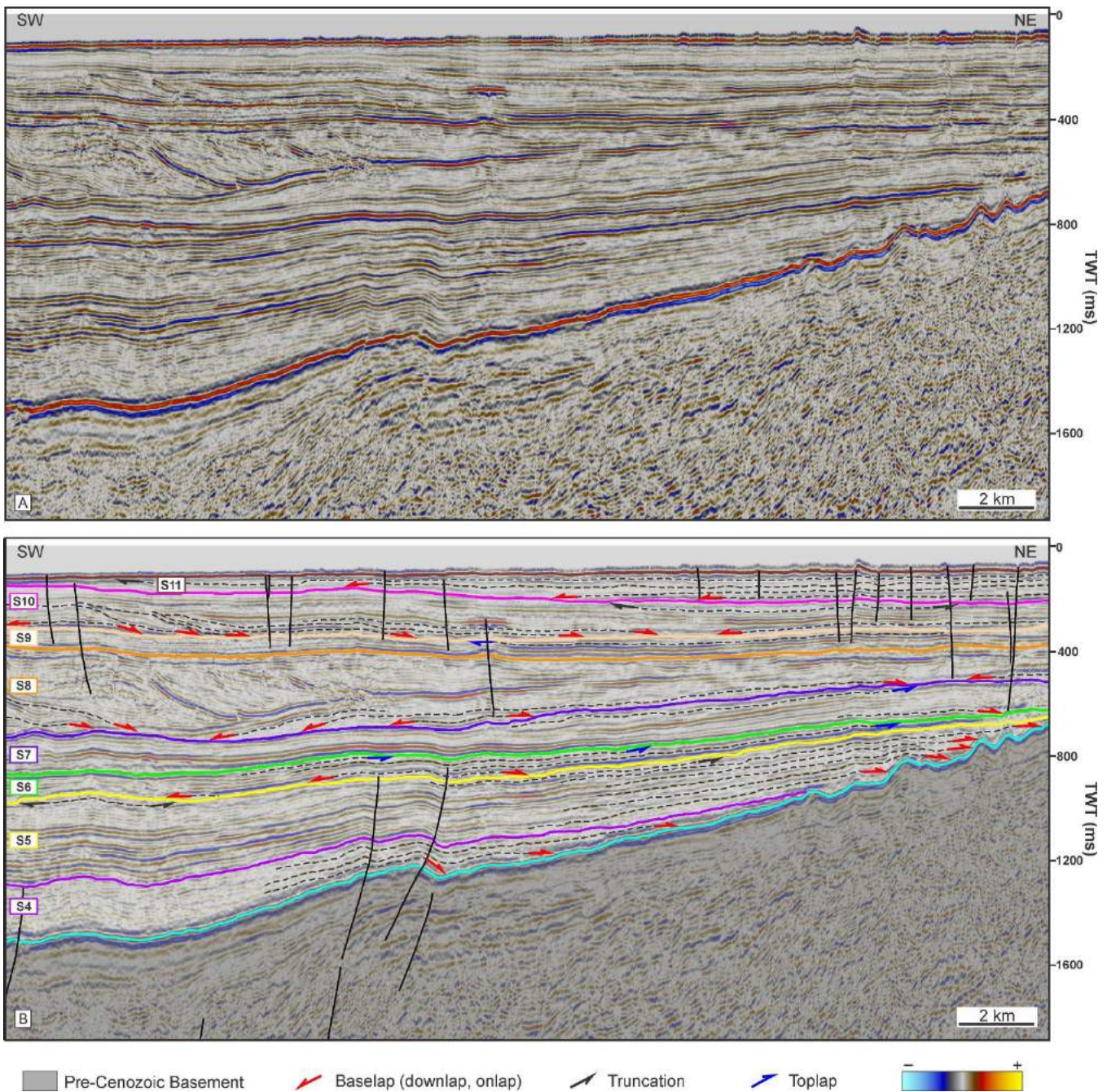


Figura 10. Reflection configuration and terminations within the Cenozoic seismic sequences. A) Uninterpreted and B) interpreted 2D seismic section across the eastern margin of the basin. The location of the seismic section is indicated in Fig. 2. Legend as in Fig. 8.

is limited to the western margin and the SWD due to it is mainly developed in the Trujillo Basin. The bulk of S1 sequence consists of hummocky reflections (SF10) that drape the SB1 topography as a wedge. To the east, SF6 grading transitionally to hummocky reflections before described (Fig. 12). To the SE, S1 sequence is condensed and sheet drapes of discontinuous reflections (SF6) are recognized. On the SWD, the S1 is characterized by SF4 reflections, and in part seismic facies are unclear due to presence of DHIs (Timoteo et al., 2015). Also westward, the S1 is punctuated by chaotic/contorted reflections (SF11) (Fig. 12, Table 1).

Seismic sequence S2

The S2 second-order sequence is bounded at its base and top by SB2 (salmon) and SB3 (light yellow), respectively. In addition, SB2 has limited distribution locally merging with SB1 thereby comprising the base of this sequence towards east (Fig. 9). Lithostratigraphically, it comprises the Heath Formation ranging in age within the Lower Miocene (~ 23 – 17 Ma) (Fig. 5). The S2 sequence onlaps the SB1 mainly over the Paracas Arch in the western margin (Fig. 9), and is absent on structural highs in southern study area (Fig. 12). The seismic signature of S2 is characterized by hummocky and discontinuous reflections (SF10 and SF6, respectively).

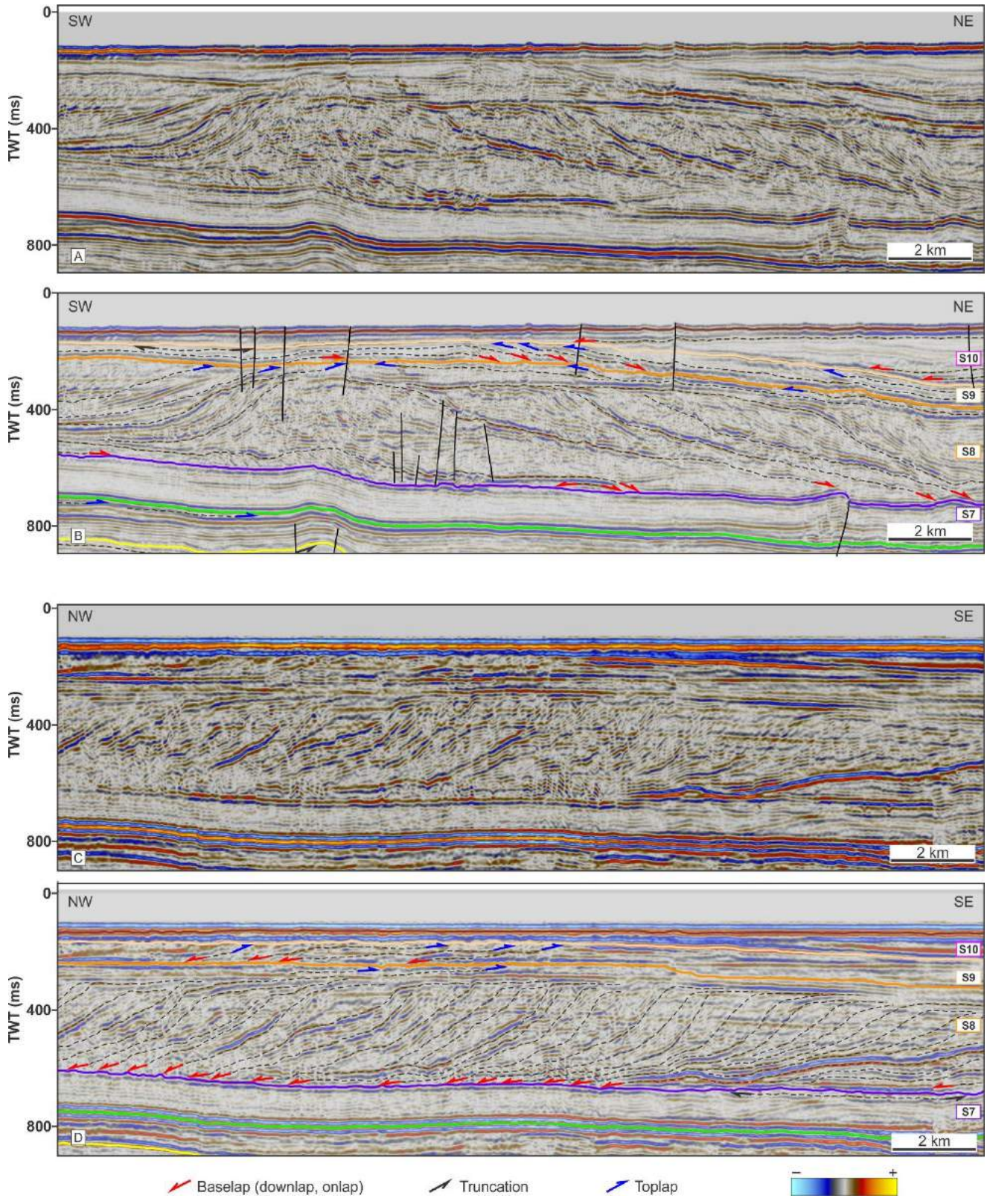


Figura 11. A) Uninterpreted and B) interpreted NE–SW seismic profile across the Cenozoic Salaverry Basin, showing the depositional strike of major delta within the S8 sequence. C) Uninterpreted and D) interpreted NW–SE seismic profile along the basin foredeep, showing the depositional dip of major delta within the S8 seismic sequence. Note the concave upward prograding clinoforms that conform the delta. Refer to Fig. 2 for location of the seismic sections. Legend as in Fig. 8.

To the east, the S2 is partly condensed grading into to SF6 reflections. In contrast, in the SWD it is dominated by SF4 and specifically on the fault zones the seismic resolution is

poor, thus the seismic facies are unclear. Westward, hummocky reflections (SF10) pass laterally to chaotic/contorted reflections (SF11) (Fig. 12, Table 1).

Seismic sequence S3

The S3 third-order sequence is bounded at its base by SB3 (light yellow) and at its top by SB4 (light blue) (Figs. 5 and 8). Well to seismic tie indicates that S3 corresponds to the lower section of Montera Formation, and ranges in age within lower Middle Miocene (~ 15.9 – 14 Ma) (Fig. 5). On the western margin and on the flanks of intrabasinal highs the S3 sequence onlaps the SB1 (Fig. 9) whereas on the SWD margins it is truncated against faults or pre-existing topography (Fig. 8C).

Internally, the S3 sequence is dominated by SF6 and SF2 reflections. Both seismic facies are organized in sheet-like geometry draping the pre-existing topography. On the eastern margin, S3 is predominantly condensed grading transitionally to SF6 and then to SF2. Likewise on the western margin, sheet and sheet drape bodies of SF10, SF3, and SF4 reflections patch the area. In addition, chaotic/contorted reflections (SF11) are observed westward (Fig. 12, Table 1).

Seismic sequence S4

The S4 third-order sequence is bounded at its base and top by SB4 (light blue) and SB5 (purple), respectively (Figs. 5 and 8). Likewise, towards the eastern margin of the basin, SB4 is overstepped by SB1, which also bounding the base of S4 sequence (Figs. 8A and B, and 10). Litostratigraphically, it comprises the upper section of Montera Formation and ranges in age within upper Middle Miocene (~ 13.6 – 11.6 Ma) (Fig. 5). The S4 onlaps the SB1 over the eastern margin, conformably overlies the deepest parts of the basin, and truncates against SB5 over the western margin (Figs. 8, 9 and 10).

The bulk of S4 seismic sequence consists of SF4 reflections that spans all over the Cenozoic Salaverry Basin. Eastward, the S4 is condensed along a narrow and continuous NW–SE fringe. This condensed portion of S4 passes laterally to SF6, and then to SF2 reflections. On the SWD margins, the seismic facies are unclear due to seismic quality decrease by faulting influence. Westward, chaotic/contorted reflections (SF11) and associated sigmoid/oblique-shaped clinofolds (SF8) are recognized. The contact between SF11 and SF2 is generally abrupt (Fig. 12, Table 1).

Seismic Sequence S5

The S5 third-order sequence is bounded at its base by SB5 (purple) and at its top by SB6 (yellow) (Figs. 5 and 8). Similar to S4 sequence towards the eastern margin of the basin SB5 is overstepped by SB1, which may therefore also bound the base of S5 sequence (Figs. 8A and B, and 10).

Well calibration shows that S5 corresponds to lower-middle section of Zapallal Formation, and ranges in age within the Upper Miocene (~ 11 – 8 Ma) (Fig. 4). The seismic signature of S5 in the main basin consists of SF4 and SF2 reflections. Along the eastern margin, SF6 reflections are organized in wedge and sheet drape bodies that conforms a continuous NW–SE fringe similar to S4 sequence. On the western margin, the S5 is characterized by divergent reflections (SF7). In addition, on the SWD margins the seismic quality is poor due to faulting, and therefore the seismic facies are unclear (Fig. 12, Table 1).

Seismic sequence S6

The S6 third-order sequence is bounded at its base and top by SB6 (yellow) and SB7 (green), respectively (Figs. 5 and 8). It comprises the upper section of Zapallal Formation and the basal section of the Miramar Formation, ranging in age from Upper Miocene to Lower Pliocene (~ 7 – 5.2 Ma) (Fig. 5). The S6 downlaps the SB6 over the western margin (Fig. 9), is conformable in the main basin (Fig. 8), and baselaps the SB6 over the eastern margin (Fig. 10).

The areal extent of S6 corresponds to almost all over the study area and only is absent over the VCB, near to the coastline (Fig. 13). SF4 reflections dominate the study area. On the eastern margin, the S6 is locally condensed grading transitionally to SF6 reflections. Some minor sheet drape bodies of SF2 and patches of SF1 are recognized towards the north and east. In addition on the western margin, divergent reflections (SF7) pass abruptly to chaotic/contorted seismic facies (SF11) (Fig. 13, Table 1).

Seismic sequence S7

The S7 third-order sequence is bounded at its base by SB7 (green) and at its top by SB8 (blue) (see the stratigraphic panel in Fig. 8). S7 has not been drilled yet in the basin (Figs. 4 and 5), thus based on seismic stratigraphic interpretation it would comprises the lower section of Miramar Formation, ranging in age within the Lower Pliocene (~ 5 – 4 Ma) (Fig. 8). The S7 predominantly rest conformable draping the pre-existing topography and only is truncated against volcanic/intrusive bodies that act as shallow morphostructural highs, on the eastern margin of the basin (Figs. 8B and 10). Wide geographic extent characterizes the S7 sequence, which only is absent over the VCB (Fig. 13).

The bulk of S7 sequence is dominated by three seismic facies consistently all over the study area: SF5 spans over the western margin; SF4 extends along the basin foredeep; and SF6 characterizes the eastern margin (Fig. 13, Table 1). For the first time in the study area, mounded reflections (SF12) are recognized as patches (~ 10 – 30 km wide) in the central part of the basin (Fig. 13, Table 1). In addition, sheet and sheet drape bodies of SF2 reflections patch considerable areas in the basin. On the other hand, the S7 seismic sequence is locally condensed eastward.

Seismic sequence S8

The S8 third-order sequence is bounded at its base and top by SB8 (blue) and SB9 (orange), respectively (see the stratigraphic panel in Fig. 8). Analogous to S7 sequence, it has not been drilled in the basin (Figs. 4 and 5) but seismic interpretation suggests that correlates to the upper section of Miramar Formation and the basal section of Hornillos Formation, ranging in age from Upper Pliocene to Lower Pleistocene (~ 3.4 – 2.2 Ma) (Fig. 8). The S8 consistently downlaps the SB8 over the study area, where the prograding clinofolds have influence (Figs. 11 and 13, Table 1).

The areal extent of S8 is very similar to S7 and S6. A major delta that progradates from SE to NW is recognized in regional seismic sections, which suggests a significant change of depositional conditions in the basin (Figs. 8B and D, and 11). Internally, the seismic signature of S8 sequence

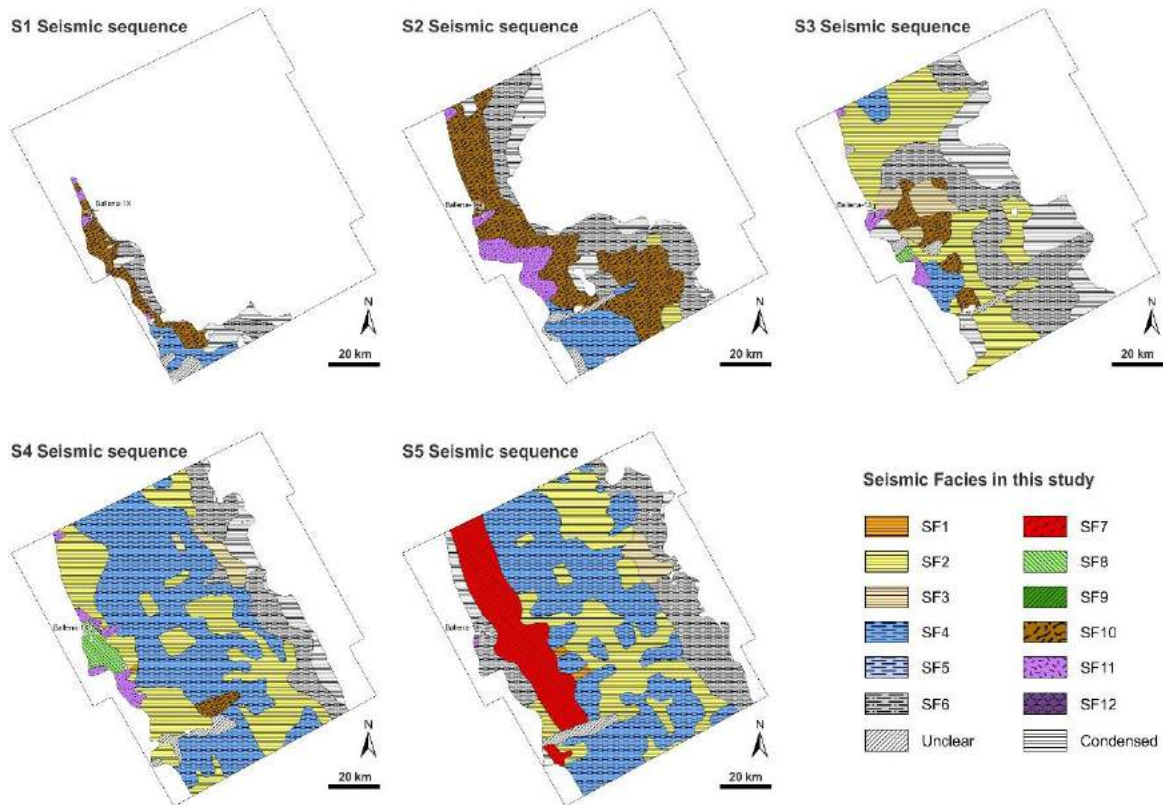


Figura 12. Seismic facies maps of the seismic stratigraphic sequences S1 to S5. Number of seismic facies in the study area (black polygon) increases from the S1 to the S11 sequences indicating that different depositional processes occurred during their deposition. See text for further explanation. See Table 1 for seismic facies description.

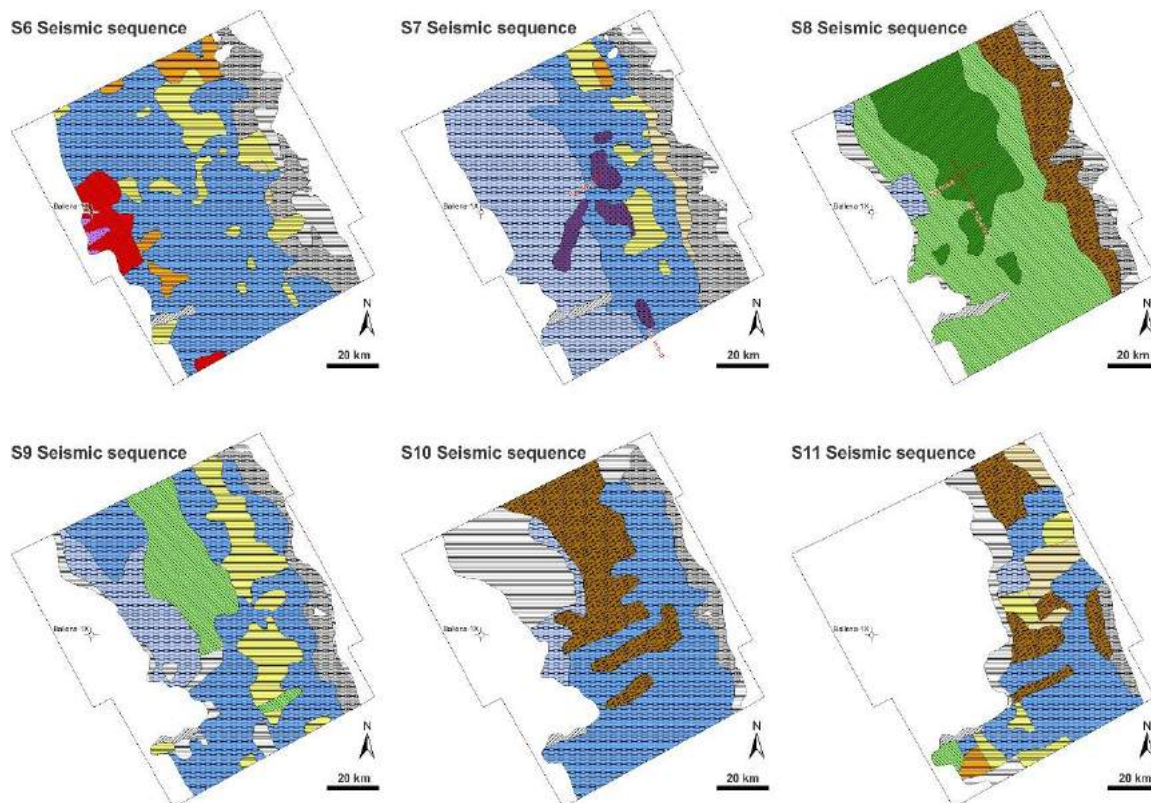


Figura 13. Seismic facies maps of the seismic stratigraphic sequences S6 to S11. See Table 1 for seismic facies description.

in the study area is characterized by different types of prograding clinoforms: sigmoid/oblique (SF8), concave upward (SF9), and hummocky (SF10) shaped reflections. Spatial-geometric relationships between these seismic facies evidence at least three major progradational events in the study area which will be studied in a subsequent paper (Fig. 13, Table 1).

Seismic sequence S9

The S9 third-order sequence is bounded at its base by SB9 (orange) and at its top by SB10 (peach orange) (see the stratigraphic panel in Fig. 8). It has not been drilled in the basin (Figs. 4 and 5) but seismic interpretation suggests that correlates to the lower section of Hornillos Formation, and ranges in age within the Lower Pleistocene (~ 2 – 1.4 Ma) (Fig. 8). The S9 baselaps consistently the pre-existing topography (Fig. 11) and locally rest conformable on the SB9 towards the eastern margin (Fig. 10).

The S9 sequence has considerable geographic extension, compared to younger sequences, and only is absent on the western margin (Fig. 13). The bulk of S9 sequence consists of SF4, SF2 and SF8 reflections. Eastward it is locally condensed grading transitionally into SF6 reflections, and then into SF4. Also, SF5 reflections are recognized to the west (Fig. 13, Table 1).

Seismic sequence S10

The S10 third-order sequence is bounded at its base and top by SB10 (peach orange) and SB11 (magenta), respectively (see the stratigraphic panel in Fig. 8). Analogous to S9 sequence, it has not been drilled in the basin (Figs. 4 and 5) but seismic interpretation suggests that correlates to the middle section of Hornillos Formation, ranging in age within the Pleistocene (~ 1.3 – 0.7 Ma) (Fig. 8). The S10 sequence baselaps consistently on the SB10 in the study area (Fig. 10).

Internally, the S10 sequence is mainly dominated by SF4 and SF10 reflections. The S10 is predominantly condensed to the northwestern sector of the study area whereas is characterized by SF6 reflections to the eastern margin, near to the coastline. Similar to S9, it is absent on the western margin of the basin (Fig. 13, Table 1).

Seismic sequence S11

The S11 third-order sequence is bounded at its base by SB11 (magenta) and at its top by SB12 (brown) (see the stratigraphic panel in Fig. 8). Similar to S7, S8, S9 and S10 it has not been drilled in the basin (Figs. 4, and 13) but seismic interpretation suggests that correlates to the upper section of Hornillos Formation, and ranges in age within Pleistocene (~ 0.6 – 0.01 Ma) (Fig. 8). The S11 sequence baselaps regionally on the SB11 (Fig. 10). The S11 geographic extent is limited to east and south sectors of the study area (Fig. 13).

The seismic signature of S11 is variable but mainly composed of parallel, continuous and disrupted in part, low to high amplitude reflections (SF4) and hummocky, low to moderate amplitude reflections (SF10). Several drape and sheet drape bodies patch the study area randomly, which are characterized by SF2, SF3, SF5 and SF1 reflections (Fig. 13, Table 1).

6. Discussion

Indeed, this study is focused in the exploration of new petroleum system elements within the entire Cenozoic succession in the central portion of the Salaverry Basin. In this way, 2D seismic data allows the recognition of twelve seismic sequence boundaries defining eleven seismic stratigraphic sequences. The integration of sequences geometry, thickness variations and seismic facies better defines the Cenozoic depositional systems and its associated potential reservoir and seal rocks. Thus, the following section describes the results and the contribution for hydrocarbon exploration in the study area.

6.1. Potential Reservoir and Seal rocks

Seismic stratigraphic analysis calibrated with available well and core data was performed to figure out depositional systems and predict lithologies. As a result, favorable reservoir facies has been interpreted into the S1, S2, S7 and S8 sequences. In addition, further data is needed to characterize potential reservoir rocks into the S4 and S5 sequences.

A) S1 Reservoir facies (Upper Eocene)

The seismic signature of S1 sequence is dominated by hummocky reflections (SF10, Table 1). Hence, the overall wedge geometry together with the consistent onlap onto the Paracas Arch from the hummocky reflections (Fig. 9) are interpreted as shallow marine sedimentation related to deltaic/shelf depositional systems (Fig. 12). S1 sequence was drilled by Ballena-1X exploratory well through the hummocky reflections described above, which correlate with packages of sandstones intercalated with claystones belonging to the Verdun Formation (Fig. 5).

Likewise, core lithofacies of Ballena-1X comprise various sandstones facies that show favorable reservoir petrographic characteristics (quartz composition, subangular to subrounded, well sorted, good visual porosity) and depict a deltaic/shelf depositional system (Fig. 14). Analogous interpretation can be derived from core lithofacies and seismic stratigraphic analysis along the hummocky seismic facies interval (SF10) drilled by Ballena-1X.

In addition, these S1 reservoir facies have 45 m (148 ft) of gross sand thickness, 21 m (69 ft) of net sand thickness, and mean gross porosity of 21% in the Ballena-1X exploratory well, showing good petrophysical properties as reservoir rocks according to Minguito et al. (1997).

B) S2 Reservoir facies (Lower Miocene)

The bulk of S2 sequence consists of hummocky and discontinuous reflections (SF10 and SF6, respectively) (Table 1). This hummocky clinoform pattern is marked by wedge and sheet draping geometry that onlap onto the Paracas Arch and the PCB (Figs. 8 and 9).

Likewise, this system dominated the basin infill during S2 time (Fig. 12) and thus suggest deltaic/shelf sedimentation likely associated with turbidity currents basinward (Fig. 12). S2 sequence was drilled by Ballena-1X exploratory well through the hummocky reflections described above, which correlate with sandstones at the base followed by

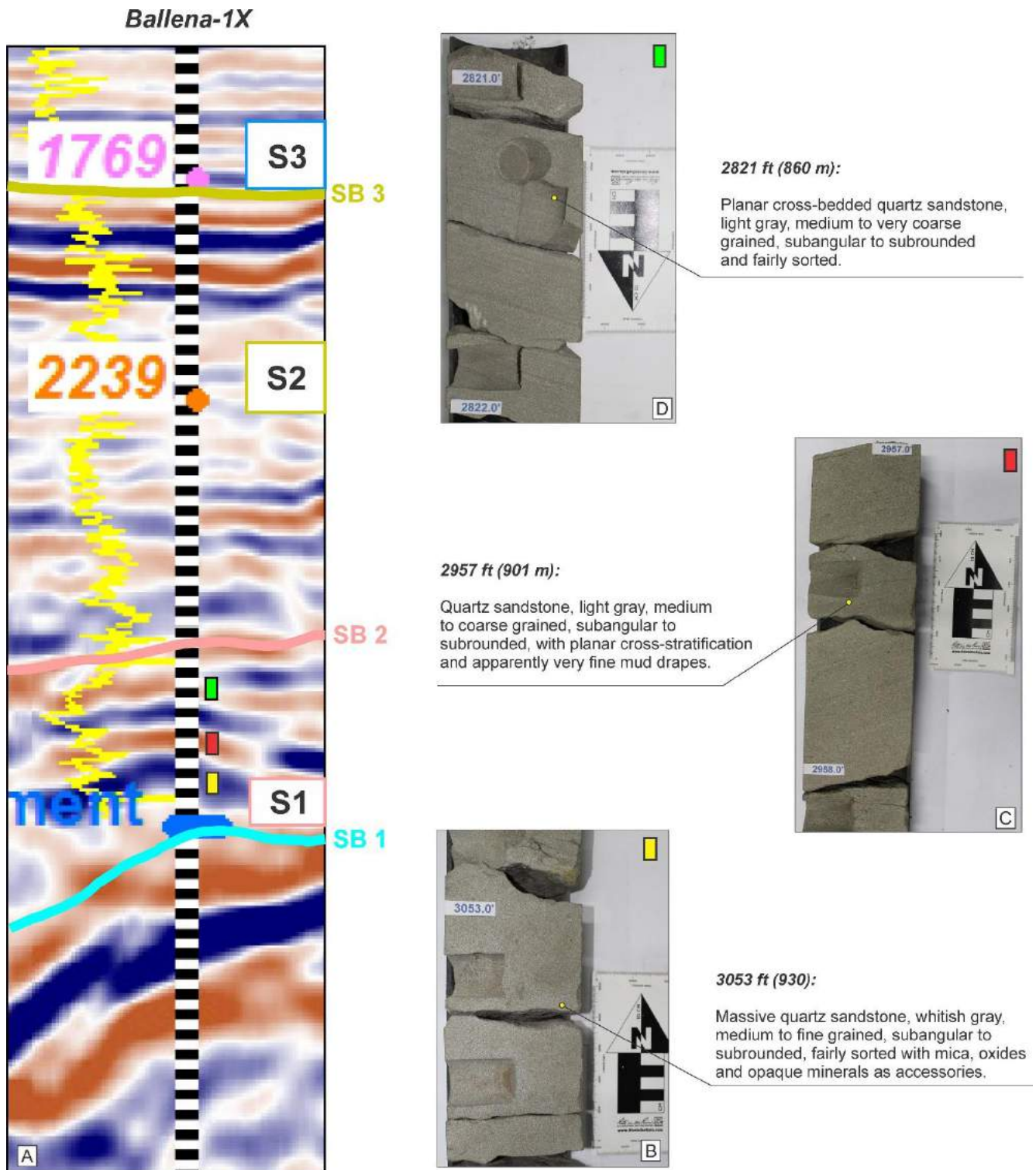


Figura 14. A) Ballena-1X seismic well tie showing the location of selected cores. B), C) and D) Core lithofacies from Ballena-1X exploratory well. Favorable reservoir facies within the S1 sequence are described. The S1 correlates to Upper Eocene Verdun Formation in the study area. Each photograph shows a graphic scale in cm.

claystones intercalated with siltstones belonging to the Heath Formation (Fig. 5). Hence, sedimentary facies described in cores from Ballena-1X, correspond to deltaic/shelf cross-bedded sandstones at the base that deepens upsection to marine claystones and siltstones interbedded with turbiditic massive sandstones (Figs. 5 and 15). These sandstones facies show good petrographic characteristics as reservoir rocks (quartz composition, subangular to subrounded, well sorted, good visual

porosity) (Fig. 15). In addition, effective integration of seismic and well data shows strong correlation in depositional system interpretation.

C) S7 Reservoir facies (Pliocene)

For the first time in the basin, into the S7 sequence have been recognized mounded reflections (SF12, Table 1) as patches (~ 10 – 30 km wide) in the central-south sectors of the study area (Fig. 13). These mounded seismic facies

bodies are interpreted as siliciclastic or carbonate? buildups due to its internal reflections are subparallel differing from cone-in-cone architecture reflections conspicuous from volcanic buildups (Figs. 16).

Interpretation of carbonate buildups must be merged with seismic interval velocity and all available geological data, given that upwelling in the offshore Peru has occurred episodically since at least the Late Eocene (Marty, 1989; Dunbar et al., 1990) favoring the temporal distribution of biogenic sediments as cool-water carbonate factory (James and Wood, 2010) in the Salaverry Basin. This kind of organic rocks may represent important reservoirs in the basin.

D) S8 Reservoir facies (Pliocene - lowermost Pleistocene)

The S8 sequence is marked by at least 3 progradational events that as whole compose a major NW-SE delta extending along the basin foredeep in the study area (Figs. 8B and D, and 11). The south-central sector of S8 is characterized by sigmoid/oblique-shaped clinoforms (SF8, Table 1), which suggest sedimentation controlled by suspension and therefore predominance of very fine-grained facies in the clinoforms (Fig. 13).

On the other hand, the central-north sector of S8 is dominated by concave upward-shaped clinoforms (SF9, Table 1), which suggest sedimentation controlled by

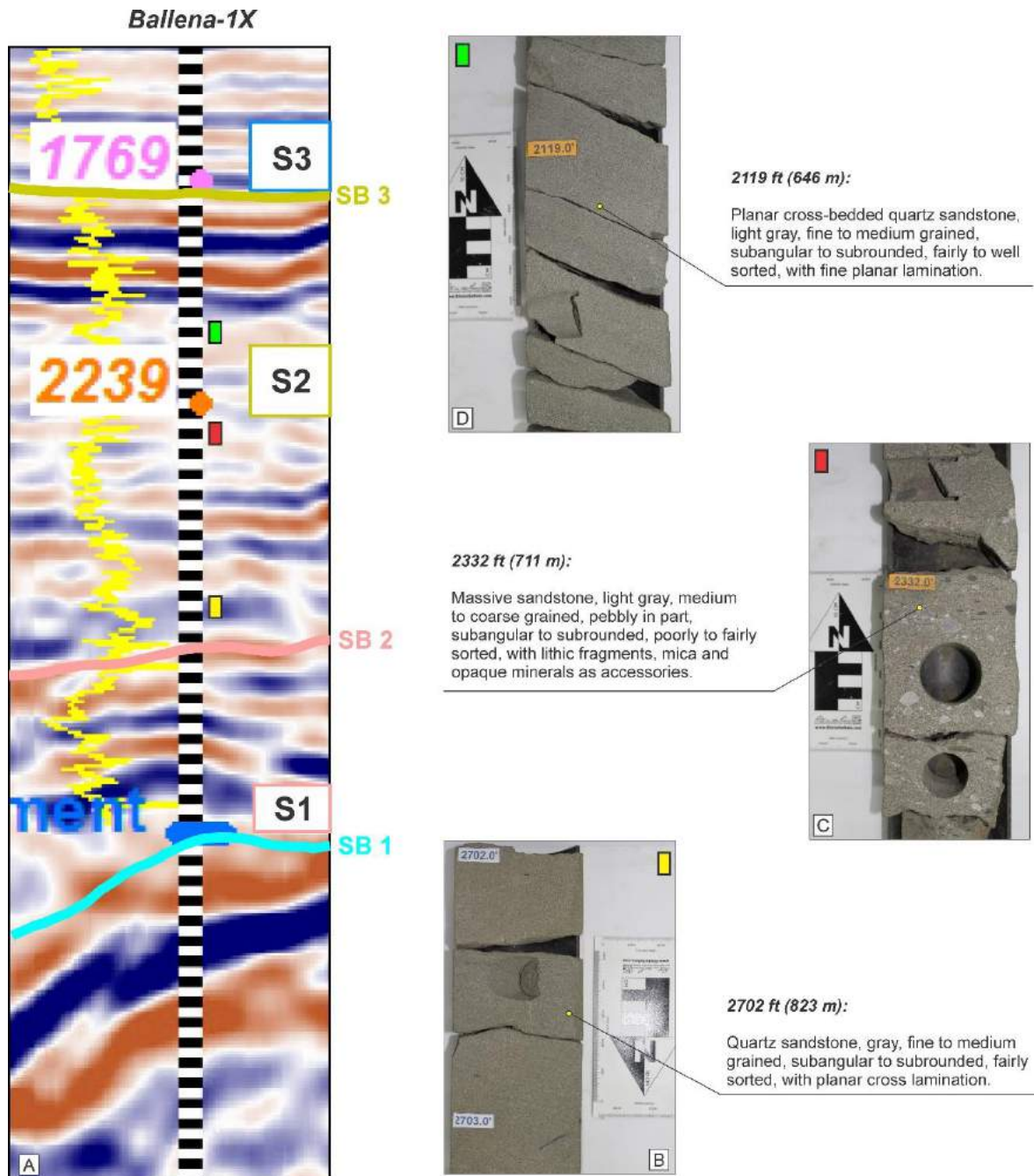


Figura 15. A) Ballena-1X seismic well tie showing the location of selected cores. B), C) and D) Core lithofacies from Ballena-1X exploratory well. Interbedded sandstones showing better conditions to potential reservoir rocks within the S2 sequence are described. The S2 correlates to Lower Miocene Heath Formation in the study area. Each photograph shows a graphic scale in cm.

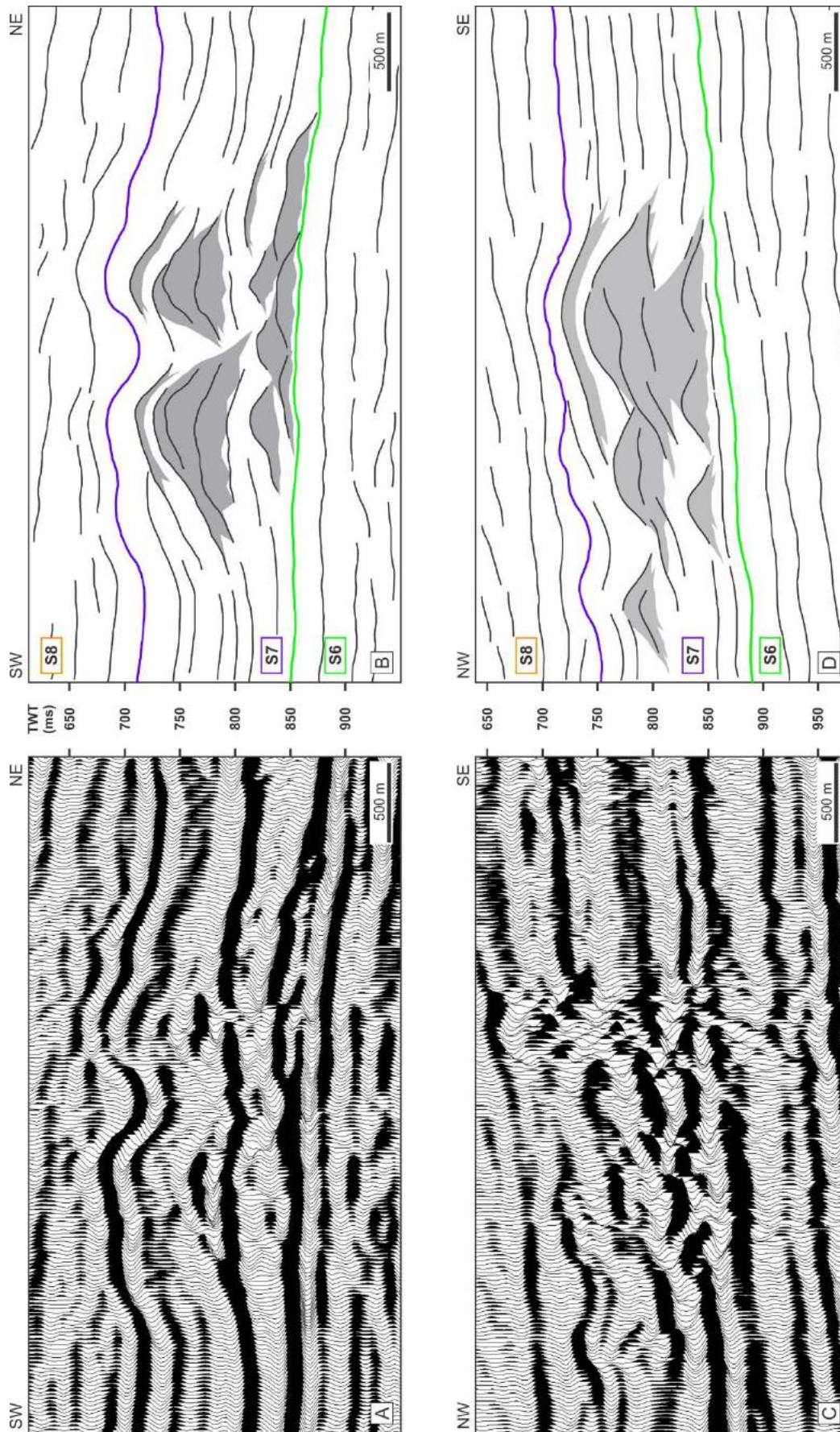


Figura 16. A) Uninterpreted and B) interpreted portion of SW-NE seismic line, showing stacked mounds (dark shading) within the S7 sequence. Note the strong impedance contrast between the mounds and surrounding sediments. C) Uninterpreted and D) interpreted portion of NW-SE seismic line, showing moderately well-defined stacked mounds (dark shading), with moderate impedance contrast with overlying sediments. Note the differential compaction over all these buildups bodies. Refer to Figs. 2 and 13 for location of seismic sections.

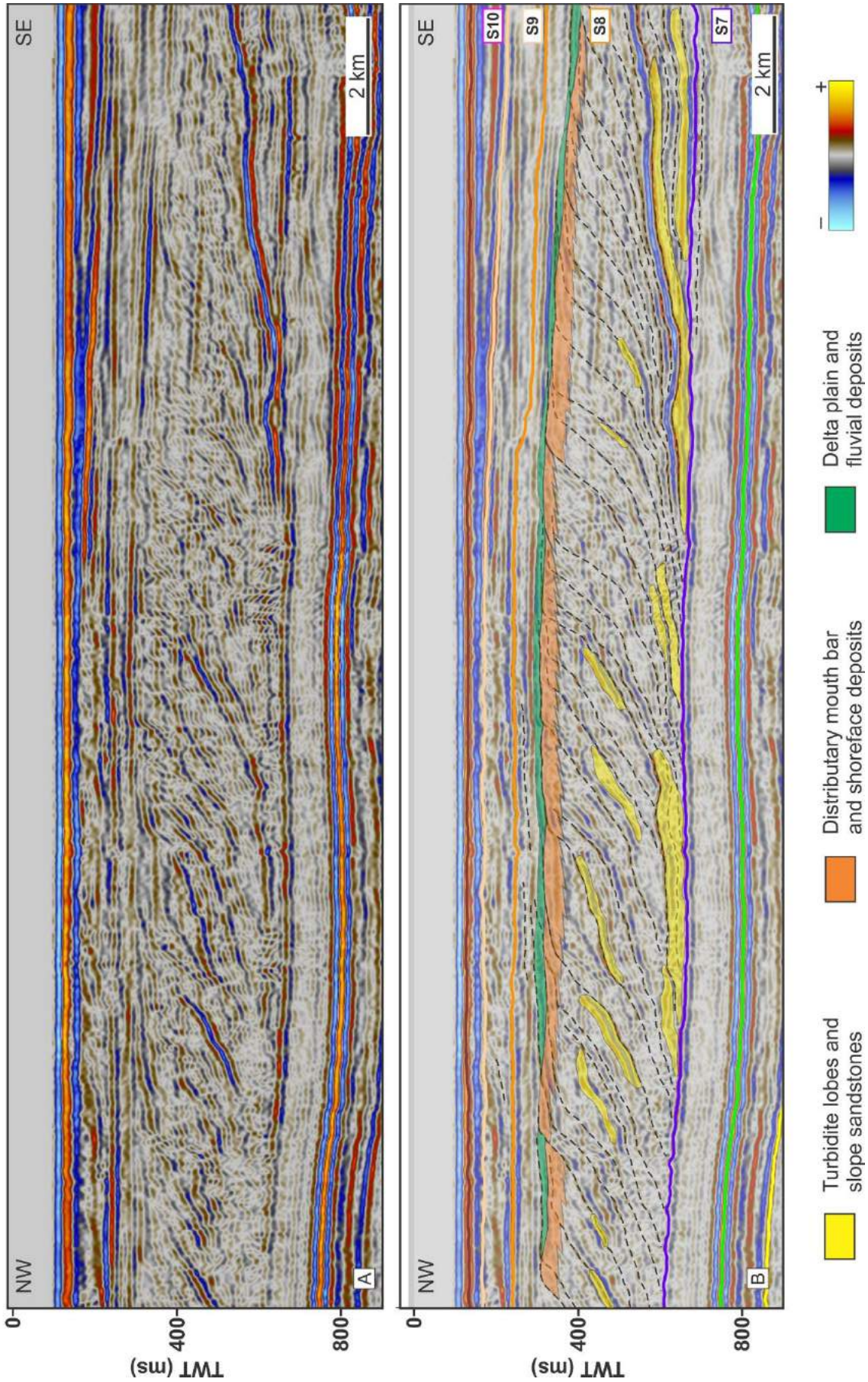


Figura 17. A) Uninterpreted and B) interpreted NW-SE seismic profile. S8 sequence shows shelfal progradation with predominantly flat trajectory. Single and clustered high amplitudes on the slope and basin floor areas suggest sand on the clinoform foresets (slope sandstones) and bottomsets (turbidite sandstones), respectively. In addition, linked distributary mouth bars and shoreface deposits are interpreted on the top of these clinoforms. The topsets would contain a mix of fluvial and coastal plain and delta plain deposits. Refer to Figs. 2 and 13 for seismic section location.

traction related to a shelfal progradation (also known as deltaic progradation) (Fig. 11). Thus, the clinoform topsets would contain a combination of delta plain and fluvial deposits whereas the clinoform tops (offlap break) are interpreted as a combination of distributary mouth bar and shoreface deposits (Fig. 17).

In addition, most clinoform foresets are interpreted as pro-delta and offshore marine deposits likely composed by shales, mudstones and siltstones. However, single and clustered high amplitude reflections in the foresets would represent slope sandstones (Fig. 17). Likewise, the clinoform bottomsets show high amplitude, baselap and lens-like external form, and are interpreted as turbidite lobes linked to the shelfal progradation (Fig. 17). Each of these turbidite lobes could host potential reservoir rocks (Figs. 13 and 17).

E) Favorable Seal facies

Seismic facies distribution from S3, S6, S9, S10 and S11 sequences are mostly characterized by parallel, continuous, variable amplitude reflections, suggesting dominance of pelagic/hemipelagic sedimentation during each sequence time (Figs. 12 and 13).

Thus, interpreted pelagic/hemipelagic deposits are predominantly comprised of shales, claystones, mudstones and siltstones, and thereby are the best place to look for regional seal rocks within the Cenozoic succession.

In addition, interpreted pro-delta/shelf deposits within S1, S2 and S8 sequences, and pelagic/hemipelagic deposits within S4, S5 and S7 sequences could host internal seal rocks for potential reservoir rocks encased within them.

7. Conclusiones

(1) The Cenozoic succession in the central portion of Salaverry Basin is best subdivided into eleven seismic stratigraphic sequences: 2 second-order sequences (S1 and S2) and 8 third-order sequences (S3–S11), controlled predominantly by tectonism and also by sea-level fluctuations.

(2) Within the S1, S2, S7 and S8 sequences have been interpreted key depositional systems that could host potential reservoir rocks:

S1: Deltaic/shelf sandstones (Upper Eocene).

S2: Deltaic and turbiditic sandstones (Lower Miocene).

S7: Siliciclastic or carbonate? buildups (Pliocene).

S8: Turbidite lobe sandstones, slope sandstones and deltaic/shoreface sandstones (Pliocene to lowermost Pleistocene).

Identification of these favorable reservoir facies may have a strong impact on exploratory activities in the Salaverry Basin. In addition, further data is needed to characterize potential reservoir rocks into the S4 and S5 sequences.

(3) Based on the integrated seismic sequence analysis, the S3, S6, S9–S11 third-order sequences would conform regional seals whereas internal seals have been

interpreted per each reservoir-sequence described in the previous point.

(4) Seismic stratigraphic analysis plays a vital role in frontier hydrocarbon exploration especially with regard to mitigating risk associated with the presence of reservoir facies. Such is the case of the Salaverry Basin in the Peruvian Forearc (west South America).

Acknowledgements

The authors acknowledge SAVIA PERU S.A. and PERUPETRO for supplying the seismic and well data, and borehole samples respectively; which made the present study possible. Diego Timoteo thanks Brazilian agency CAPES for graduate Scholarship.

References

- Alemán, A. 2006. Collision of aseismic ridges in Perú. Backbone of the Americas Symposium, Geological Society of America and Asociación Geológica Argentina. Abstracts with Programs, Special Meeting 2, Mendoza, p. 21.
- Azalgara, C. 1993. Structural evolution of the offshore forearc basins of Peru, including the Salaverry, Trujillo, Lima, West Pisco and East Pisco basins. A Thesis submitted in partial fulfillment of the requirements for the degree Master of Arts. Rice University – Houston, Texas.
- Benavides, V. 1999. Orogenic evolution of the Peruvian Andes: the Andean cycle. In: Skinner, B. (Ed.), *Geology and Mineral Deposits of Central Andes*. Society of Economic Geology, Special Publication, vol. 7, pp. 61–108.
- Canchanya, Z., Paz, M. 1992. Estudio Bioestratigráfico en base a nannoplancton calcáreo: pozo Delfin-1X y Ballena-1X, Cuenca Salaverry. Petroperu, unidad de investigación y desarrollo. Reporte interno Petroperu.
- Clift, P.D., Pecher, I., Kukowski, N., Hampel, A. 2003. Tectonic erosion of the Peruvian forearc, Lima Basin, by subduction and Nazca Ridge collision. *Tectonics*, vol. 22(3), pp. 1023. Doi:10.1029/2002TC001386.
- Deckelman, J.A., Connors, F.X., Shultz, A.W., Glagola, P.A., Menard, W.M., Schwegal, S.R., Shearer, J.N. 2008. Neogene Oil and Gas Reservoirs in The Progreso Basin, Offshore Ecuador And Peru: Implications for Petroleum Exploration and Development. *Journal of Petroleum Geology*, vol. 31, pp. 43–60.
- Dunbar, R.B., Marty, R.C., Baker, P.A. 1990. Cenozoic marine sedimentation in the Sechura and Pisco Basins, Peru. *Palaeogeography, Palaeoclimatology, Palaeoecology*, Vol. 41, pp. 235–261.
- Gonzales, E., 2014. Biostratigraphy Chart Salaverry Basin – Chan Area: based on microfossils (planktonic, benthonic, nanno, pollen and spores). Savia Peru S.A. Internal Report.
- Gutscher, M.A., Spakman, W., Bijwaard, H., Engdahl, E.R. 2000. Geodynamic of flat subduction: seismicity and tomographic constraints from the Andean margin. *Tectonics*, vol. 19, pp. 814–833.
- Hampel, A. 2002. The migration history of the Nazca Ridge along the Peruvian active margin: A re evaluation. *Earth Planetary Science Letters*, 203, pp. 665–679.

- James, N.P. and Wood, R. 2010. Reefs, In: James N. P. and Dalrymple, R.W., (eds) *Facies Models 4. Geological Association of Canada, GEOText 6*, pp. 421-447.
- Johannessen, E.J., and Steel, R.J. 2005. Shelf-margin clinofolds and prediction of deep water sands. *Basin Research*, vol. 17, pp. 521-550.
- Kulm, L.D., Prince, R.A., French, W., Johnson, S., Masias, A. 1981. Crustal structure and tectonics of the central Perú continental margin and trench. *Geological Society of America, Memoir 154*, 445-508.
- Martinez, E., Fernandez, J., Calderón, Y., Hermoza, W., Galdos, C. 2005. Tumbes and Talara Basins Hydrocarbon Evaluation. Exploration Department, Basin Evaluations Group. Perupetro Internal report.
- Marty, R.C. 1989. Stratigraphy and chemical sedimentology of Cenozoic biogenic sediments from the Pisco and Secura Basins, Peru. Doctoral Thesis, Rice University. <http://hdl.handle.net/1911/16267>.
- Minguito, M.A., Machín, J., Cakebread, J., Beroiz, C. 1997. Hydrocarbon Potential Review. Z-29 block, Trujillo basin, Perú. Volume I: Geology. Repsol Exploración S.A. Internal Report.
- Mitchum, R.M., Vail, P.R., Sangree, J.B. 1977. Seismic stratigraphy and global changes of sea level, Part 6: Stratigraphic interpretation of seismic reflection patterns in depositional sequences. In: Payton, C.E. (Ed.), *Seismic Stratigraphy – Applications to Hydrocarbon Exploration*. American Association of Petroleum Geologists, Memoir 26, pp. 117-135.
- Morales, C., Gonzales, E. 2006. Determinación litológica y bioestratigráfica de los pozos Ballena-1X, Delfin-1X, Lobos-1X y Morsa-1X, Cuenca Trujillo. Petro-tech Peruana Internal Report.
- Narvaez, J., Pardo, A. 1993. Nueva fauna fósil del Eoceno del pozo Delfin-1X (Margen continental, norte del Perú): Alcances estratigráficos y tectónicos. Reporte interno Petroperu.
- Okada, H. 1990. Nannofossils biostratigraphy of the Ballena-1X and Delfin-1X wells. In: Azalgará, C. (Msc Thesis), *Structural Evolution of the Offshore Forearc Basins of Peru, Including the Salaverry, Trujillo, Lima, West Pisco and East Pisco Basins*. Appendix A.
- Peña, D. 2011. Geología del Cenozoico – Cuenca Salaverry. Savia Perú Reporte Interno.
- Ramos, V.A., Alemán, A. 2000. Tectonic evolution of the Andes. In: Cordani, U.J., Milani, E.J., Thomaz Filho, A., Campos, D.A. (Eds.), *Tectonic Evolution of South America, 31° International Geological Congress, Rio de Janeiro*, pp. 635- 685.
- Ramos, V.A. 2014. Evolución Tectónica Paleozoica de los Andes Peruanos: Nuevos datos y nuevas hipótesis. Instituto de Estudios Andinos (Universidad de Buenos Aires – CONICET). Conferencia Magistral, XVII Congreso Geológico Peruano, Lima-Perú.
- Ramsayer, G.R. 1979. Seismic stratigraphy, a fundamental exploration tool: 11th Annual Offshore Technology Conference Proceedings, p. 101-109.
- Romero et. al. 2010. Evolución Tectono-sedimentaria del margen continental durante el Jurásico-Cretácico, costa afuera del Perú Central. XV Congreso Peruano de Geología. Resúmenes Extendidos. Sociedad Geológica del Perú. Publicación Especial N° 9.
- Romero, D., Valencia, K., Alarcón, P., Ramos, V.A. 2011. Geología de la costa pacífica del Perú central entre Chiclayo y Paracas (7_e14_ Sur). 14 Congreso Latinoamericano de Geología, Memorias, Medellín, pp. 110-111.
- Romero, D., Valencia, K., Alarcón, P., Peña, D. and Ramos, V.A. 2013. The offshore basement of Perú: Evidence for different igneous and metamorphic domains in the Forearc. *Journal of South American Earth Sciences*, vol. 42, pp. 47-60.
- Rosenbaum, G., Giles, D., Saxon, M., Betts, P.G., Weinberg, R.F., Duboz, C. 2005. Subduction of the Nazca Ridge and the Inca Plateau: Insights into the formation of ore deposits in Peru. *Earth Planet. Sci. Lett.*, 239, 18 – 32. Doi:10.1016/j.epsl.2005.08.003.
- Sangree, J.B., Widmier, J.M. 1977. Seismic stratigraphy and global changes of sea level, Part 9: Seismic interpretation of clastic depositional facies. In: Payton, C.E. (Ed.), *Seismic Stratigraphy – Applications to Hydrocarbon Exploration*. American Association of Petroleum Geologists, Memoir 26, pp. 165-184.
- Schell, W. W. 1978. Paleontology Occidental Wells, Peru. Occidental Petroleum Company Internal Report.
- Schrader, H., and Cruzado, J. 1990. The Ballena and Delfin wells off central Peru: revised ages. In Suess, E., von Huene, R., et al., *Proc. ODP, Sci. Results, Vol. 112: College Station, TX (Ocean Drilling Program)*, pp. 209-215. <http://dx.doi.org/10.2973/odp.proc.sr.112.187.1990>.
- Snedden, J. W., Sarg, J. F. 2008. *Seismic Stratigraphy – A Primer on Methodology*. AAPG Search and Discovery Article #40270.
- Steel, R.J., Carvajal, C., Petter, A. and Urosa, C. 2008. Shelf and shelf margin growth in scenarios of rising and falling sea level. In: *Recent Advances in Models of Siliciclastic Shallow-marine Stratigraphy* (ed. By G.J. Hampson, P.M. Burgess, R.J. Steel et al.). Society of Economic Paleontologists and Mineralogists, Special Publication, vol. 90, pp. 47-71.
- Timoteo, D. 2013. Potencial Generador de Hidrocarburos y Distribución de las Secuencias Cretácicas costa afuera (offshore) del Perú centro-norte (Lima – Chiclayo). Tesis para optar el Título Profesional de Ingeniero Geólogo. UNI, Lima- Perú.
- Timoteo, D. 2015. Sismoestratigrafia dos Depósitos Cenozoicos da Bacia Salaverry, porção offshore do Peru: Novas interpretações do sistema petrolífero. Dissertação de Mestrado N 356. Instituto de Geociências. Programa de pós-graduação em Geologia. Universidade de Brasília, Brasília.
- Vail, P.R., Mitchum, R.M., Thompson, S. 1977. Seismic stratigraphy and global changes of sea level, Part 3: Relative changes of sea level from coastal onlap. In: Payton, C.E. (Ed.), *Seismic Stratigraphy – Applications to Hydrocarbon Exploration*. American Association of Petroleum Geologists, Memoir 26, pp. 83-98.
- Vail, P. R. 1987. Seismic Stratigraphy Interpretation Using Sequence Stratigraphy: Part 1: Seismic Stratigraphy Interpretation Procedure. In *Atlas of Seismic Stratigraphy* (A. W. Bally, Ed.), pp. 1-10. American Association of Petroleum Geologists Studies in Geology No 27.

- Valdespino, T., Seminario, F. 1976a. Informe Micropaleontológico del pozo Ballena 8X-1. Reporte interno Petroperu.
- Valdespino, T., Seminario, F. 1976b. Informe Micropaleontológico del pozo Delfin 20X-1X. Reporte interno Petroperu.
- Valencia, K., and Romero, D. 2011. Evolución Tectono-sedimentaria de la Cuenca Salaverry y su Implicancia en la Generación de Hidrocarburos. VII Seminario Internacional de Exploración y Producción de Petróleo y Gas - INGEPET Perupetro S.A. Lima- Perú.
- Valencia, K., Romero, D., Alarcón, P., Llerena, C., Borda, E., and Rojas, J. 2013. Structural Evolution of Convergent Margin of Central Peru and its Relationship with Petroleum Systems of the Forearc Salaverry Basin. AAPG Search and Discovery Article #90166.
- Veeken, P.C. 2013. Seismic Stratigraphy and Depositional Facies Models. EAGE Publications, pp. 467.
- Von Huene, R., and Scholl, D. W. 1991. Observations at convergent margins concerning sediment subduction and the growth of continental crust. *Rev. Geophys.*, 29, 279 - 316, 1991.
- Wine, G., Arcuri, J., Martínez, E., Monges, C., Calderón, Y., Galdos, C. 2001. Hydrocarbon Potential of the Salaverry Offshore Basin Peru. Perupetro Internal Report.
- Witt, C.A., Alarcón, P., Valencia, K., Lajo, A., Fuentes, J., Romero, D. 2011. Segmentación tectono-estratigráfica y superposición de cuencas de antearco cenozoicas en la margen andina entre 6°S y 2°S (Norte Perú e Sur Ecuador). 14 Congreso Latinoamericano de Geología, Memorias, Medellín, pp. 248-249.